Vol. 12, No. 1, March 31, 2021
Since 2010

ISSN 2233-4203 (print)
e-ISSN 2093-8950

Mass Spectrometry Letters

Mass Spectrometry Letters
Vol. 12, No. 1, March 31, 2021
The Korean Society for Mass Spectrometry

A Dilute-and-Shoot LC–MS/MS Method for Screening of 43 Cardiovascular Drugs in Human Urine

KSMS Korean Society for Mass Spectrometry

Mass Spectrometry Letters

ISO Abbreviation: *Mass Spectrom. Lett.*
Websites: www.msletters.org; msletters.koar.kr

Editorial Office
Administration office of the Korean Society for Mass Spectrometry
78 Daejeon Dunsan P.O.Box, 111 Dunsan-ro, Seo-gu, Daejeon, 35239, Republic of Korea
Contact: Yae Jin Joo
Homepage: www.ksms.org
E-mail: ksms@ksms.org
Tel: 82-70-8688-1696
Fax: 82-43-240-5159

Editor-in-Chief: Jeongkwon Kim, Ph.D.
E-mail: jkkim48105@cnu.ac.kr
Phone: 82-42-821-5477
Department of Chemistry
Chungnam National University
Republic of Korea

Manuscript Editor: Ki Hwan Choi, Ph.D.
E-mail: kihwan.choi@kriss.re.kr
Phone: 82-42-868-5557
Korea Research Institute of Standards and Science
Republic of Korea

MASS SPECTROMETRY LETTERS is indexed in Academic Society Village (http://society.kisti.re.kr), NDSL (National Discovery for Science Leaders, http://www.ndsl.kr), KSCI (Korea Science Citation Index, http://ksci.kisti.re.kr), KCI (Korea Citation Index, http://www.kci.go.kr), Chemical Abstracts (http://cas.org), and Scopus (www.scopus.com).

The journal hardcopy is distributed free to all the KSMS members who pay the membership fee in the corresponding year or at the cost of 20 US dollars/year to non-members.

Subscription information
Mass Spectrometry Letters follows ‘OPEN ACCESS’policy. One who wants to have an access to the full text is recommended to visit the Mass Spectrometry Letters official website (http://www.msletters.org/).
The printed material is sent to all the members of the KSMS for free and anyone who wants to receive the printed journal in Korea is strongly recommended to enroll in the KSMS. The membership fee information can be found in the KSMS homepage (www.ksms.org). One who wants to receive the printed journal abroad should contact Yae Jin Joo for more information.

Mass Spectrometry Letters Vol. 12, No. 1

Printed on March 25, 2021
Published on March 30, 2021

Publisher: Young Hwan Kim, President of KSMS
Publication Office: The Korean Society for Mass Spectrometry
Published since December 2010
Frequency of publication: 4 issues/year
The number of circulation of the printed journal: 400 copies/issue
Printed by Hanrimwon, Seoul, Korea, Tel: 82-2-2273-4201
ISSN 2233-4203 (print)
e-ISSN 2093-8950

Aims and Scope

Mass Spectrometry Letters publishes brief letters (maximum length of 4 pages), technical notes, articles, reviews, and tutorials on fundamental research and applications in all areas of mass spectrometry. The manuscripts can be either invited by the editors or submitted directly by authors to the journal editors. Mass Spectrometry Letters topical sections are diverse, covering ion chemistry in a broad sense; gas-phase thermodynamics or kinetics; theory and calculations related with mass spectrometry or ions in vacuum; ion-optics; analytical aspects of mass spectrometry; instrumentations; methodology developments; ionization methods; proteomics and its related research; metabolomics and its related research; bioinformatics; software developments; database development; biological research using mass spectrometry; pharmaceutical research by mass spectrometry; food sciences using mass spectrometry; forensic results using mass spectrometry; environmental mass spectrometry; inorganic mass spectrometry; chromatography-mass spectrometry; tandem mass spectrometry; small molecule research using mass spectrometry; TOF-SIMS, etc. The scope of Mass Spectrometry Letters is not limited to the above-mentioned areas, but includes ever-expanding areas related directly or indirectly to mass spectrometry. Criteria for publication are originality, urgency, and reportable values. Short preliminary or proof-of-concept results, which will be further detailed by the following submission to other journals, are recommended for submission.

CONTENTS

Volume 12, Number 1
March 2021

ARTICLE

Vol. 12, No. 1, 2021
ISSN 2233-4203/ e-ISSN 2093-8950
ARTICLE www.msletters.org | Mass Spectrometry Letters

A Dilute-and-Shoot LC–MS/MS Method for Screening of 43 Cardiovascular Drugs in Human Urine

Thuy-Vy Pham[1#], Gunhee Lee[1#], Xuan-Lan Mai[2], Thi-Anh-Tuyet Le[1], Thi Ngoc Van Nguyen[3], Jongki Hong[4], and Kyeong Ho Kim[1]*

[1]*College of Pharmacy, Kangwon National University, Chuncheon 24341, Korea*
[2]*Faculty of Pharmacy, Ho Chi Minh City University of Technology (HUTECH), Ho Chi Minh, Vietnam*
[3]*Faculty of Pharmacy, Can Tho University of Medicine and Pharmacy, Can Tho, Vietnam*
[4]*College of Pharmacy, Kyung Hee University, Seoul, Korea*

Received December 22, 2020, Revised Feburary 8, 2021, Accepted Feburary 24, 2021
First published on the web March 31, 2021; DOI: 10.5478/MSL.2021.12.1.1

Abstract : A simple, specific, and economical LC–MS/MS method was investigated for the screening of 43 prescribed antihypertensive and related drugs in human urine. The urine samples were simply prepared by diluting and mixing with internal standard before directly introduced to the LC-MS/MS system, which is fast, straightforward, and cost-effective. Fractional factorial, Box-Behnken, and I-optimal design were applied to screen and optimize the mass spectrometric and chromatographic factors. The analysis was carried out on a triple quadrupole mass spectrometer system utilizing multiple reaction monitoring with positive and negative electrospray ionization method. Chromatographic separation was performed on a Thermo Scientific Accucore RP-MS column (50 × 3.0 mm ID., 2.6 μm) using two separate gradient elution programs established with the same mobile phases. Chromatographic separation was performed within 12 min. The optimal method was validated based on FDA guideline. The results indicated that the assay was specific, reproducible, and sensitive with the limit of detection from 0.1 to 50.0 μg/L. The method was linear for all analytes with coefficient of determination ranging from 0.9870 to 0.9981. The intra-assay precision was from 1.44 to 19.87% and the inter-assay precision was between 2.69 and 18.54% with the recovery rate ranges from 84.54 to 119.78% for all drugs measured. All analytes in urine samples were stable for 24 h at 25°C, and for 2 weeks at -60°C. The developed method improves on currently existing methods by including larger number of cardiovascular medications and better sensitivity of 12 analytes.

Keywords : antihypertensive drugs, screening test, dilute-and-shoot LC-MS/MS, experimental design

Introduction

Hypertension and other cardiovascular diseases which have been among the leading cause of death worldwide, are preventable and manageable by medications such as antihypertensive, hypolipidemic, or anticoagulant agents.[1] However, the increasing of non-adherence to antihypertensive and related drugs is a real menace to patient health and drug effectiveness. Several conventional methods have been applied to evaluate medication adherence including questionnaires, pharmacy dispense records, pill counts, or supervised administration.[2] Besides, recently, drug testing in urine, oral fluid, or plasma using liquid chromatography tandem mass spectrometry (LC-MS/MS) has been proven as a valuable means for assessing the adherence of prescribed medications. The developed LC-MS/MS methods for drug adherence monitoring in general and studying cardiovascular medications in particular generally applied sample preparation processes employed solid-phase extraction or liquid-liquid extraction.[3-8] This approach effectively cleans up and concentrates the analytes but significantly depends on the characteristics of the surveyed compounds as well as consumes labor, reagents, and time Nowadays, the enhancement in the sensitiveness of LC–MS/MS systems have allowed samples to be minimally diluted and then directly introduced into the analytical system. This offers a simple and faster sample preparation process (about 30 s) with minimal labor, time and reagent consumption and be able to screen the broader range of analytes in comparison to other mentioned techniques. For instance, “dilute-and-shoot” LC-MS/MS has been proven as an effective trend in doping

#These authors contributed equally in this study
*Reprint requests to Kyeong Ho Kim, orcid.org/0000-0002-1298-8277
E-mail: kyeong@kangwon.ac.kr

control,[9] analytical toxicology,[10] or urine drug testing of a large number of antipsychotics, opioids, benzodiazepines, and other pain management medications and metabolites.[11-13] As such, a limited number of antihypertensive, lipid-lowering, antihyperglycemic, antithrombotic and other cardiovascular agents were successfully screened in urine applying "dilute-and-shoot" LC-MS/MS method.[14-16] In which, the study of A.J. Lawson covered a largest number of antihypertensive medications but only 23 compounds.[14]

From the above overview, this study developed a "dilute-and-shoot" LC-MS/MS method to detect a larger number of cardiovascular preventive compounds, covering 43 prescribed antihypertensive, lipid-lowering, and antithrombotic agents available worldwide. The design of experiment (DOE) was aslo applied through the method development process to achieve the effectively and reliably optimal LC-MS/MS condition with minimum experiments, time, cost, and labor consumption.[17]

Experimental

Material

43 surveyed cardiac drugs as well as atenolol-d7, and sulfameter (as internal standards (IS)) were provided from Sigma-Aldrich (St. Louis, MO, USA). Other IS including amlodipine-d4, clopidogrel-d4, diltiazem-d3, losartan-d4, telmisartan-d7 were supplied by TLC Pharmaceutical Standard. Formic acid, ammonium formate, HPLC-grade acetonitrile, and methanol were purchased from Daejung (Siheung, South Korea). Distilled water was prepared in the laboratory utilizing an Aqua Max water purification system supplied by Young Lin Instrument Co., Ltd. (Anyang, South Korea).

Instrumentation

The LC-MS/MS system included an Agilent 1200 series (Agilent Technologies) system combined with an API 3200 Q Trap triple-quadrupole mass spectrometer (AB SCIEX) operated with a Turbo V Ion Spray source. Analyst 1.6 software was employed for LC-MS/MS system management and data processing. The separation was performed on a Thermo Scientific Accucore RP-MS column (50 × 3.0 mm ID., 2.6 μm) combined with a C18 guard column (Phenomenex, 4.0 × 3.0 mm ID), both maintained at 50°C. Two separate gradient elution programs established with the same mobile phases: eluent A containing 8mM ammonium formate ($HCOONH_4$) and 0.1% formic acid (HCOOH) in water, and eluent B containing 8mM $HCOONH_4$ and 0.1% HCOOH in acetonitrile (ACN): water (90:10).

Drug calibrators and quality control samples preparation

A 1 mg/mL stock solution in methanol was made for each compound measured and IS, with the exception of 2 mg/mL for nicotinic acid and 5 mg/mL for HCTZ. Therefore, the concentration of nicotinic acid and HCTZ is correspondingly 2 times and 5 times higher than that mentioned the following solutions. Working standard mixtures of 4000 μg/L, 200 μg/L, 10 μg/L and IS working standard mixtures of 4000 μg/L were prepared by serial dissolving the stock solutions in water. All solutions were keeped at -20°C and thawed at room temperature (25°C) before use. Fifteen calibration standards (0.25, 0.5, 1, 2, 5, 10, 20, 30, 50, 100, 200, 400, 600, 800, 1000 μg/L) were prepared by spiking an appropriate volume of the diluted standard solutions into an aliquot containing 250 μL of drug free human urine, and 200 μL of diluted IS solution, followed by dilution with water to attain a total volume of 1000 μL. Quality control (QC) samples correspond with three concentration levels (low, medium, and high) were independently prepared in the same way for all drugs measured. The sample was then vortexed and filtered using 0.45 μm filter before introducing into LC-MS/MS system.

MS analyte parameters

Precursor and product ion transitions of each compound were determined by direct infusion of standard solution with positive and negative electrospray ionization (ESI) source. The multiple reaction monitoring (MRM) transitions and compound tuning parameters are shown in Table 1. According to optimization results, the optimal mode for each compound which created the higher intensity signal was selected (i.e. 39 compounds were detected in a positive ESI method and 4 compounds in a negative ESI method).

In scouting phase, five MS parameters including ion spray voltage, capillary temperature, curtain gas, ion source gas 1, and ion source gas 2 were screened to identify the significant factors by applying fractional factorial design. Peak areas of poorly sensitive compounds (Amlodipine, Atenolol, Captopril, Losartan, Lovastatin, Moxonidine, Nicotinic acid, and Spironolactone) were chosen as responses. Analysis of variance (ANOVA) was utilized to assess the impacts of factors. Selected important factors were then optimized by Box-Behnken design with 15 runs including 3 centre points.

LC parameters

As the analytical column is stable at temperature below 60°C, the influence of the column temperature was studied in a range from 20°C to 50°C with a step of 5°C. Three LC related parameters namely flow rate, ammonium formate concentration, and percentage of eluent B at 0 min were also optimized by I-optimal design with 20 runs. Intensities of poor sensitive compounds were chosen as responses.

Method validation

Selectivity

The selectivity of method was studied by comparing six

drug-free urine samples from six individual sources and drug-free urine samples spiked with a surveyed medications mixture at lower limit of quantification (LLOQ) concentrations. The absence of interfering peaks at retention times of analytes indicated satisfactory selectivity.

Sensitivity

The limit of detection (LOD) was assessed by the analyte concentration with the signal-to-noise (S/N) ratio was > 3. The LLOQ concentration was determined at which the S/N ratio was ≥ 10 as well as the precision (assessed by relative standard deviation, RSD) and variance of accuracy (relative error, RE) were ≤ 20%.

Carryover

The carryover was tested by analyzing the blank samples right away the upper limit of quantification (ULOQ) samples (n = 3). The carryover should ideally be < 20%.

Matrix effect

The matrix factors of the analytes were assessed by comparing the analyte/IS ratio in urine samples and water (solvent) at low, medium, and high concentration in three separate experiments (n = 3). Average percentage difference between the two should preferably be between -20% and 20%.

Linearity

The linearity was tested within the concentration range from LLOQ to ULOQ concentration using a weighting factor of 1/x in the linear regression analysis. Linearity was evaluated basing on the coefficient of determination (R^2) in five replicates. R^2 value of >0.95 indicated acceptable linear.

Table 1. MRM transitions, Compound tuning parameters, and t_R.

Compound	Q1	Q3 (1)	Q3 (2)	ESI	DP (V)	EP (V)	CE1 (V)	CE2 (V)	t_R (min)	IS
Acebutolol	337.2	116.3	56.2	(+)	56	7	27	47	1.85	Ate7
Amlodipine	410.2	239.2	238.2	(+)	21	4	17	17	4.55	Aml4
Aspirin	178.8	93.0	93	(-)	-15	-3.5	-8	-32	4.50	Los4
Atenolol	267.2	145.2	56.2	(+)	26	10	37	41	0.85	Ate7
Atorvastatin	559.4	440.4	250.3	(+)	66	8.5	23	53	5.12	Clo4
Bendroflu-methiazide	420.0	289.1	197.1	(-)	-80	-4.5	-24	-66	5.35	Los4
Betaxolol	308.2	55.1	72.2	(+)	61	6	45	33	4.28	Tel7
Bevantolol	346.2	165.2	150.2	(+)	56	6.5	25	43	4.27	Aml4
Bisoprolol	326.2	116.3	74.1	(+)	51	5.5	23	37	3.98	Tel7
Captopril	218.1	116.1	75.1	(+)	36	7.5	17	27	1.65	Ate7
Carvedilol	407.2	100.0	56.2	(+)	56	7	41	63	4.42	Aml4
Celiprolol	380.2	74.2	251.3	(+)	51	6.5	47	27	3.40	Sul
Clonidine	230.0	74.1	124.0	(+)	56	8.5	101	57	1.00	Ate7
Clopidogrel	322.1	155.2	184.3	(+)	36	4.5	47	33	5.69	Clo4
Diltiazem	415.2	178.2	109.2	(+)	46	5.5	33	85	4.26	Dil3
Doxazosin	452.2	344.4	247.3	(+)	106	10	33	51	4.12	Dil3
Enalapril	377.3	234.3	91.1	(+)	41	6	23	75	4.12	Tel7
Fluvastatin	412.2	354.4	354.5	(+)	66	6.5	19	19	5.12	Clo4
Furosemide	329.0	205.0	284.9	(-)	-45	-4.5	-24	-14	5.02	Los4
Hydrochlorothiazide (HCTZ)	296.6	77.7	270.1	(-)	-50	-5	-48	-14	1.78	Sul
Indapamide	366.1	132.2	91.2	(+)	46	6.5	23	53	4.41	Dil3
Irbesartan	429.2	207.1	205.2	(+)	56	7	31	69	4.83	Tel7
Labetalol	329.2	91.1	162.2	(+)	36	6.5	53	31	3.84	Dil3
Lisinopril	406.2	84.2	91.1	(+)	56	6.5	41	87	0.83	Sul
Losartan	424.2	208.2	207.3	(+)	51	5	27	33	4.69	Los4
Lovastatin	405.3	199.3	173.2	(+)	56	5.5	21	25	5.54	Clo4
Metoprolol	268.2	74.1	56.2	(+)	46	9	33	43	2.13	Sul
Mevastatin	391.3	185.2	159.3	(+)	56	5	25	33	5.40	Tel7
Moxonidine	243.2	207.2	200.1	(+)	66	8	19	27	0.71	Ate7

Table 1. Continued.

Compound	Q1	Q3 (1)	Q3 (2)	ESI	DP (V)	EP (V)	CE1 (V)	CE2 (V)	t_R (min)	IS
Nadolol	310.2	254.3	201.3	(+)	51	6	21	27	1.00	Ate7
Nicotinic acid	124.0	80.1	78.1	(+)	46	10	29	29	0.71	Sul
Olmesartan	559.2	207.2	190.3	(+)	71	6	37	103	4.69	Los4
Perindopril	369.2	172.3	98.1	(+)	46	6	25	49	4.23	Tel7
Pindolol	249.2	116.3	172.2	(+)	46	9	23	21	1.14	Ate7
Pitavastatin	422.2	274.3	290.3	(+)	91	7	61	31	4.83	Dil3
Propranolol	260.2	116.3	56.1	(+)	51	7.5	23	43	4.12	Dil3
Ramipril	417.2	234.3	91.2	(+)	76	5.5	25	91	4.41	Dil3
Rosuvastatin	482.3	258.1	258.3	(+)	81	5	37	37	4.69	Tel7
Spironolactone	341.2	107.2	91.2	(+)	76	7	41	73	4.97	Clo4
Telmisartan	515.2	276.3	261.3	(+)	96	8	65	83	4.83	Tel7
Terazosin	388.1	290.3	247.3	(+)	76	9.5	29	35	1.42	Ate7
Triamterene	254.2	237.3	104.2	(+)	76	12	33	51	1.02	Ate7
Warfarin	309.1	163.1	251.2	(+)	71	6	19	23	4.97	Tel7
Amlodipine-d4	413.2	238.2	298.3	(+)	66	5	19	19	4.41	
Atenolol-d7	274.3	145.2	79.2	(+)	51	6.5	35	33	0.71	
Clopidogrel-d4	326.1	216.2	159.2	(+)	51	6	19	45	5.54	
Diltiazem-d3	418.1	178.1	109.1	(+)	46	6	31	85	4.27	
Losartan-d4	427.2	211.3	210.2	(+)	60	5	43	45	4.55	
	425.1	128	157.2	(-)	-60	-4.5	-40	-36	5.43	
Sulfameter	281.1	65	108.1	(+)	51	5.5	65	33	1.71	
	279	196.1	264.1	(-)	-45	-4.5	-38	-12	3.02	
Telmisartan-d7	522.3	280.4	279.3	(+)	111	12	63	67	4.83	

DP: de-clustering potential, EP: entrance potential, CE: collision energy, t_R: Retention time

Precision and accuracy

The intra-day, inter-day precisions, and accuracy were assessed by analyzing five replicates on same day, and over three different days of four concentrations: LLOQ, low of quantification (LQC), medium of quantification (MQC), and high of quantification (HQC). Standard curves for each batch were prepared and analysed on the same day to determine the concentration of each QC sample. RSD and RE were also calculated to evaluate the precision and accuracy.

Stability

The stability of all compounds in urinary samples was investigated at 3 QC concentrations (LQC, MQC, and HQC) in three replicates. The QC samples were stored under 4 different storage conditions before analyzing: 24 h at room temperature (25°C), 2 weeks at -20°C, three cycles of freezing (-60°C for 12 h) and thawing (room temperature), and autosampler 5°C for 24 h. An analyte was considered to be stable in urine when the calculated concentrations were 85–115% of those of the freshly prepared samples.

Results

Method development

Preliminary experiments were conducted with the following gradient LC condition proposed by Lawson et al.: eluent A including 1mM $HCOONH_4$ and 0.1% HCOOH in water, and eluent B including 1mM $HCOONH_4$ and 0.1% HCOOH in 90% ACN.[14] Some analytes such as captopril, losartan, lovastatin, moxonidine, nicotinic acid, hydrochlorothiazide (HCTZ) or spironolactone showed the poor sensitivity and chromatographic performance, so further experiments were conducted to obtain the more suitable condition.

Optimization of MS parameters

At first, five MS parameters including ion spray voltage, capillary temperature, curtain gas, ion source gas 1, and ion source gas 2 were screened to identify the significant factors by applying fractional factorial design. Since p-value < 0.05, ion spray voltage, capillary temperature, and curtain gas were demonstrated the more importance and selected for optimization step. These MS selected factors

Table 2. The optimization of MS parameters.

		Negative mode	Positive mode
Factors & ranges	Ionspray voltage (V)	-4500 ~ -3500	3000 ~ 5000
	Temperature (°C)	450 ~ 650	450 ~ 650
	Curtain gas (psi)	30 ~ 50	20 ~ 40
Responses		Peak areas of Aspirin, Bendroflumethiazide, Furosemide, HCTZ	Peak areas of Amlodipine, Atenolol, Captopril, Losartan, Lovastatin, Moxonidine, Nicotinic acid, Spironolactone
Total run		15 runs	15 runs
Desirability value		0.954	0.427
Optimal MS values	Ionspray voltage (V)	-4500	4207
	Temperature (°C)	650	637
	Curtain gas (psi)	50	20
	Ion source gas 1 (psi)	60	60
	Ion source gas 2 (psi)	30	70

were optimized by Box-Behnken design with 15 runs including 3 centre points. From the results of Box-Behnken design, optimal MS conditions were revealed. The desirability values were 0.954 and 0.427 for negative and positive mode, respectively (Table 2).

Optimization of LC parameters

The results of column temperature investigation showed that high temperatures faster elution of analytes, improved peak shapes, and obtained the acceptable sensitivity (peak area and peak height). Therefore, the temperature of analytical column was stabled at 50°C in following experiments.

Three other LC related parameters namely flow rate, ammonium formate concentration, and percentage of eluent B at 0 min were also optimized by I-optimal design with 20 runs. Intensities of poor sensitive compounds were chosen as responses. At optimal condition, the desirability values were 0.943 and 0.466 for negative and positive mode, respectively (Table 3).

Overall, there were the significant differences in desirability values between positive and negative mode since the number of responses of positive mode (8) was higher than that of negative one (4). Despite the low desirability, the sensitivity and chromatographic performance of almost surveyed compounds was acceptable and good enough for drug screening method. Therefore, the finally optimal LC-MS/MS was selected following DOE results (Table 2 and 3). The complete chromatograms all analytes were shown in Figure 1.

Method validation

Selectivity and sensitivity

There were no considerable interfering peaks observed at the retention times expected for the analytesf or IS. The extracted ion chromatograms of 43 interested compounds and IS were shown in Supporting Information (Figure S1).

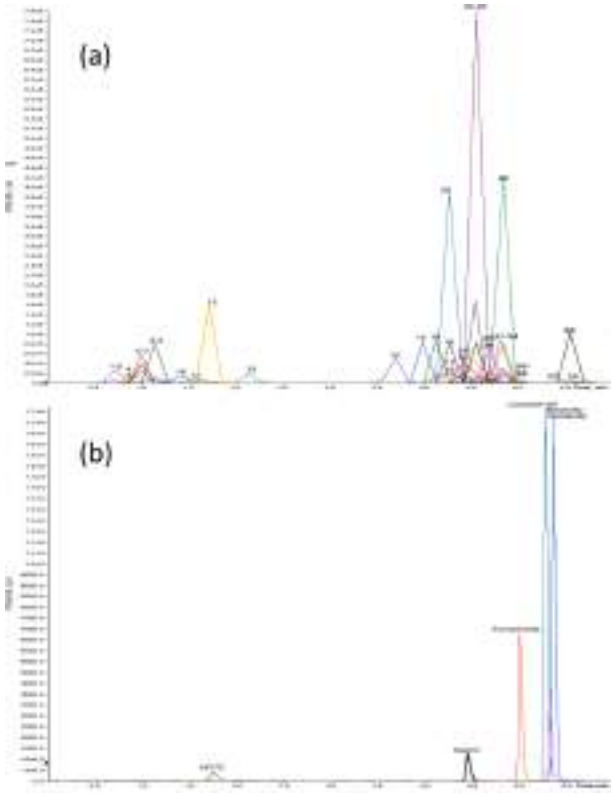

Figure 1. Chromatograms of 40 analytes in a positive ESI mode (a) and 4 analytes in a negative ESI mode (b): 1. Moxonidine, 2. Nicotinic acid, 3. Atenolol, 4. Lisinopril, 5. Clonidine, 6. Nadolol, 7. Triamterene, 8. Enalapril, 9. Pindolol, 10. Terazosin, 11. Captopril, 12. Acebutolol, 13. Metoprolol, 14. Celiprolol, 15. Labetalol, 16. Bisoprolol, 17. Doxazosin, 18. Propranolol, 19. Perindopril, 20. Diltiazem, 21. Bevantolol, 22. Betaxolol, 23. Indapamide, 24. Ramipril, 25. Carvedilol, 26. Amlodipine, 27. Losartan, 28. Olmesartan, 29. Rosuvastatin, 30. Irbesartan, 31. Pitavastatin, 32. Telmisartan, 33. Spironolactone, 34. Warfarin, 35. Atorvastatin, 36. Fluvastatin, 37. Mevastatin, 38. Lovastatin, 39. Clopidogrel.

Table 3. The optimization of LC condition.

		Negative mode	Positive mode
Factors & ranges	Flow rate (mL/min)	0.3 – 0.5	0.3 – 0.5
	Buffer conc. (mM)	2 - 8	2 - 8
	%B at 0 min (%)	10 - 30	10 - 30
Responses		(Similar to MS parameters optimization)	
Total run		20 runs	20 runs
Desirability value		0.943	0.466
Optimal LC condition	Flow rate (mL/min)	0.3	0.37
	Buffer conc. (mM)	8	8
	%B at 0 min (%)	10	15
	Gradient elution - Eluent A: 8 mM $HCOONH_4$ and 0.1% HCOOH in Water - Eluent B: 8 mM $HCOONH_4$ and 0.1% HCOOH in Water - ACN (1:9)	0.0–0.2 min: 10%B 0.2-2.5 min: 10% – 100%B 2.5-6.0 min: 100%B 6.0-7.0 min: 100% – 10%B 7.0-12.0 min: 10%B	0.0–0.2 min: 15%B 0.2-2.5 min: 15% – 100%B 2.5-6.0 min: 100%B 6.0-7.0 min: 100% – 15%B 7.0-12.0 min: 15%B

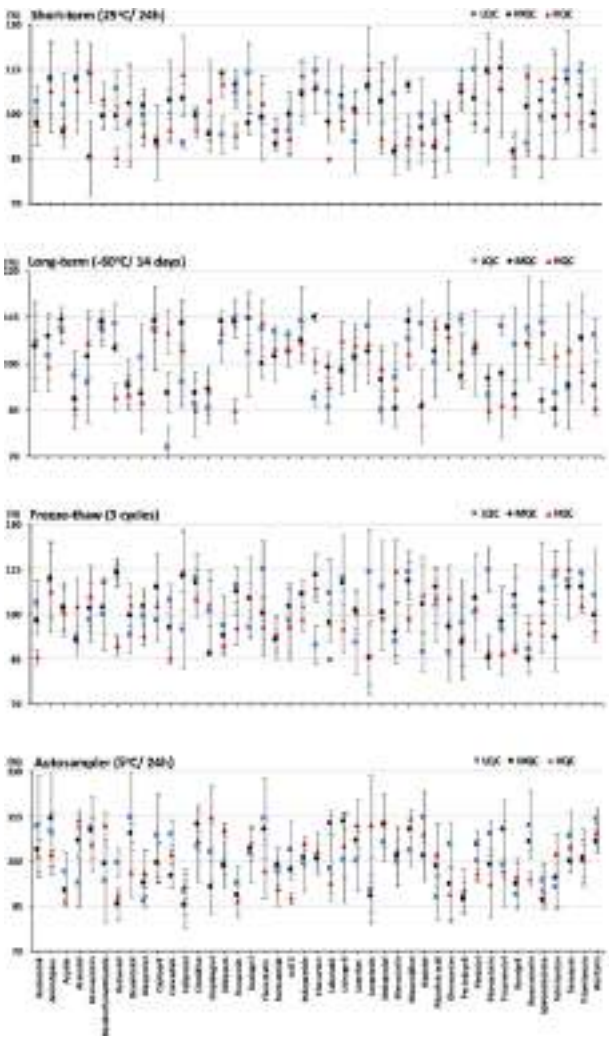

Figure 2. Stability validation.

The LODs were from 0.1 to 50 ppb, and the LLOQs ranged from 0.25 to 100 ppb (Table 4).

Carryover

The carryover of the all surveyed compounds was less than 19.48% of the LLOQ (Table 4).

Matrix effect

Mean percentage difference of the analyte/IS ratio between human urine and water samples was from -19.92% to 18.92% for all but three analytes (bevantolol, carvedilol, nicotinic acid) (Table 4).

Linearity

The coefficient of determination (R^2) of all compounds was more than 0.9870 showing the acceptable linearity of the developed method.

Precision and accuracy

The good precision and accuracy were observed for all compounds (Table 5). The RSD% was not more than 19.87% and 18.54% for intra-assay and inter-assay precision, respectively. The recovery of each compound was in the range from 84.54 to 119.78%.

Stability

The results of stability validation are shown in Figure 2 and Supporting Information (Table S1). Under four storage conditions, the mean of recoveries and RSD satisfied the acceptance criteria (± 15% of the control values) for all analytes but carvedilol (recovery of 73.07% at LQC). No significant degradation was detected, so most analytes were assessed to be stable in urine under all described conditions.

Table 4. QC concentrations, sensitivity, linearity, carry over, matrix effect validation.

Compound	**LOD** (ppb)	**LLOQ** (ppb)	LQC (ppb)	MQC (ppb)	HQC (ppb)	ULOQ (ppb)	R^2	Carry over (%)	Matrix effect (%)		
									LQC	MQC	HQC
Acebutolol	0.25	1	3	100	400	600	0.9901	9.61	-7.98	-6.53	-10.49
Amlodipine	5	10	30	200	600	800	0.9935	16.13	-5.18	-1.62	-3.13
Aspirin	10	20	60	160	800	1000	0.9954	7.82	-12.88	-10.00	-6.26
Atenolol	5	20	60	200	800	1000	0.9907	3.83	12.71	0.76	-4.83
Atorvastatin	5	10	30	200	600	800	0.9935	6.67	18.06	5.38	-7.49
Bendro-flumethiazide	1	2	6	120	600	800	0.9958	6.38	0.61	7.28	3.03
Betaxolol	5	10	30	200	600	600	0.9931	12.51	13.16	0.43	9.94
Bevantolol	0.25	0.5	1.5	50	100	200	0.9934	19.48	-0.92	-21.12	-30.43
Bisoprolol	0.5	2	6	100	400	600	0.9915	8.43	-18.73	13.11	18.92
Captopril	1	2	6	100	400	600	0.9977	0.00	5.69	9.61	-14.08
Carvedilol	10	30	90	200	800	1000	0.9913	4.14	-42.68	-5.16	-3.95
Celiprolol	0.1	0.25	0.75	20	100	100	0.9870	13.04	10.74	7.56	7.02
Clonidine	0.5	2	6	100	400	600	0.9958	10.02	-0.47	7.50	-7.09
Clopidogrel	1	2	6	100	400	600	0.9966	12.72	-4.35	-19.91	-19.68
Diltiazem	0.25	1	3	100	400	600	0.9956	13.32	-1.45	-1.85	9.88
Doxazosin	1	5	15	100	400	800	0.9956	11.11	-10.33	-13.86	-11.55
Enalapril	0.1	0.5	1.5	50	400	600	0.9965	4.19	-13.18	-14.97	14.43
Fluvastatin	10	20	60	200	800	1000	0.9901	0.00	0.74	0.13	14.21
Furosemide	5	10	30	160	800	1000	0.9974	16.49	-12.88	-13.62	-7.21
HCTZ	50	100	300	800	4000	5000	0.9912	1.89	-13.53	0.22	-12.83
Indapamide	2	5	15	100	400	600	0.9899	16.21	10.72	-5.14	-8.89
Irbesartan	0.25	0.5	1.5	50	400	600	0.9949	17.56	-7.20	-14.24	-10.38
Labetalol	5	10	30	200	600	600	0.9908	12.62	16.89	8.10	18.69
Lisinopril	5	10	30	200	600	800	0.9920	2.83	-6.46	-1.34	8.39
Losartan	0.5	2	6	100	400	400	0.9872	14.83	4.31	-6.41	5.17
Lovastatin	2	10	30	200	600	600	0.9961	11.13	1.00	1.57	5.15
Metoprolol	0.25	0.5	1.5	50	400	400	0.9937	5.38	-3.26	-3.89	-15.46
Mevastatin	1	5	15	100	400	600	0.9936	13.12	18.40	11.00	12.93
Moxonidine	2	5	15	100	400	600	0.9933	5.34	12.78	-1.19	-4.26
Nadolol	0.5	1	3	100	400	400	0.9968	12.31	7.44	9.96	7.34
Nicotinic acid	50	100	300	800	1600	2000	0.9908	15.65	12.20	-44.78	-57.56
Olmesartan	0.25	1	3	100	400	600	0.9967	6.01	-3.24	-18.21	-11.91
Perindopril	0.25	1	3	100	400	600	0.9981	16.64	5.16	-1.73	12.64
Pindolol	0.1	0.25	0.75	20	100	100	0.9960	13.57	-2.38	18.02	4.80
Pitavastatin	0.25	0.5	1.5	50	100	200	0.9931	7.02	8.87	-6.10	1.03
Propranolol	2	10	30	200	600	600	0.9934	10.17	7.35	-4.53	-6.42
Ramipril	0.25	0.5	1.5	200	600	600	0.9969	17.20	-11.42	-0.23	-10.06
Rosuvastatin	5	10	30	200	600	600	0.9948	17.60	4.97	-19.92	-6.15
Spironolactone	10	30	90	200	800	1000	0.9938	9.76	-4.59	7.75	12.40
Telmisartan	1	5	15	100	400	600	0.9937	18.88	-17.32	1.78	-12.96
Terazosin	0.1	0.5	1.5	50	400	400	0.9922	10.84	-6.14	15.30	15.13
Triamterene	0.5	2	6	100	400	600	0.9944	6.14	-10.40	-11.75	0.57
Warfarin	2	5	15	100	400	600	0.9927	14.96	-13.62	-13.91	-12.69

Table 5. Precision, and accuracy results.

Compound	Intra-day (n = 5)								Inter-day (n = 3)							
	LLOQ		LQC		MQC		HQC		LLOQ		LQC		MQC		HQC	
	RE %	RSD %	RE %	RSD %	RE %	RSD %	RE %	RSD %	RE %	RSD %	RE %	RSD %	RE %	RSD %	RE %	RSD %
Acebutolol	109.14	19.73	113.00	4.77	106.72	7.09	103.24	7.07	103.82	18.21	110.75	8.65	107.22	7.27	95.68	5.80
Amlodipine	85.14	19.41	86.52	12.23	104.56	12.10	110.96	11.77	100.41	18.30	94.97	11.79	100.56	11.47	100.77	10.67
Aspirin	99.44	7.15	94.42	6.94	92.74	7.47	93.62	3.88	109.35	4.40	97.91	7.13	95.63	7.38	91.31	4.05
Atenolol	103.84	7.81	112.00	2.45	98.72	5.08	105.60	5.46	112.68	9.75	106.42	7.44	99.69	3.83	98.05	4.87
Atorvastatin	118.74	15.20	102.74	7.26	90.20	6.32	95.30	2.67	119.57	14.73	106.03	8.70	94.57	7.57	94.09	2.69
Bendroflu-methiazide	110.94	8.80	101.66	14.41	93.74	6.80	93.3	3.50	105.62	12.12	97.23	10.98	94.66	6.77	94.40	6.34
Betaxolol	104.24	7.82	108.80	6.08	92.54	3.14	85.94	5.07	101.95	9.30	106.73	8.01	100.41	6.16	86.89	4.14
Bevantolol	115.00	13.00	112.80	5.59	100.24	11.91	89.74	2.94	113.87	14.28	114.27	8.50	101.71	10.21	90.29	8.30
Bisoprolol	103.14	15.87	97.48	12.50	107.02	7.27	105.60	1.44	108.11	13.75	103.43	10.04	100.85	7.84	104.57	5.04
Captopril	115.90	12.26	113.02	14.78	113.80	1.44	108.60	3.10	112.72	9.99	106.93	12.96	105.21	6.63	94.90	7.23
Carvedilol	94.90	10.68	85.14	5.12	100.00	12.76	93.60	5.85	101.09	8.07	104.59	5.71	105.60	7.83	105.67	7.19
Celiprolol	119.78	17.80	88.14	14.68	101.88	10.82	107.06	7.16	119.21	18.54	91.87	14.13	99.16	11.26	101.78	9.43
Clonidine	104.80	11.99	102.78	12.51	95.08	8.49	92.72	3.34	111.92	12.39	108.41	9.33	104.99	10.49	93.94	4.88
Clopidogrel	91.68	9.18	99.26	11.61	97.68	11.96	113.40	3.61	107.71	13.25	101.30	10.83	96.75	9.14	113.15	5.29
Diltiazem	95.26	15.01	86.90	14.04	105.12	7.52	107.20	1.79	102.51	14.31	100.30	11.03	106.70	5.80	108.27	5.78
Doxazosin	111.94	14.83	102.26	12.46	105.46	6.60	102.16	3.52	114.63	13.95	101.13	10.36	102.07	4.70	99.77	5.21
Enalapril	115.42	19.13	97.92	9.15	90.40	6.75	88.74	4.80	109.75	16.75	98.73	13.39	94.93	6.58	98.92	4.32
Fluvastatin	118.00	14.43	112.36	13.63	95.26	13.36	89.32	5.44	118.14	15.24	111.33	11.30	94.49	9.20	96.17	6.10
Furosemide	96.92	10.86	96.14	1.48	97.38	6.31	105.6	2.28	98.81	11.48	97.41	5.06	93.48	6.87	95.96	5.23
HCTZ	106.66	12.31	99.42	10.68	104.12	8.12	96.06	4.88	101.85	11.84	99.82	9.88	100.74	7.66	94.09	6.24
Indapamide	117.96	19.36	104.58	8.06	106.88	7.32	106.60	3.15	112.88	15.47	109.96	12.17	103.27	6.65	109.87	3.70
Irbesartan	109.10	8.01	108.12	8.80	113.80	6.73	110.60	4.17	98.36	12.70	93.83	10.99	104.66	4.56	101.31	4.71
Labetalol	84.54	14.45	89.32	14.56	89.42	11.09	85.74	8.03	101.13	13.84	97.31	9.84	105.47	6.86	97.91	7.00
Lisinopril	115.98	10.74	109.40	2.93	108.00	4.86	115.00	7.22	108.77	9.93	102.10	5.42	105.51	7.88	103.81	7.30
Losartan	108.38	7.17	107.66	12.45	108.58	14.95	96.82	9.70	109.56	13.49	105.38	12.19	100.44	12.61	90.41	8.84
Lovastatin	111.26	17.11	85.66	11.34	97.60	8.56	106.00	14.82	102.61	17.25	94.25	9.48	89.87	11.16	107.91	13.77
Metoprolol	112.74	19.22	102.78	14.11	95.98	7.97	99.72	4.07	114.42	16.96	96.15	11.51	101.89	8.82	98.80	6.69
Mevastatin	113.40	12.16	98.14	10.63	95.84	10.60	106.08	10.60	108.06	13.58	96.35	11.14	93.77	11.88	102.53	11.65
Moxonidine	119.52	19.19	104.56	11.34	109.20	2.37	95.72	5.58	113.79	17.27	106.43	13.25	110.47	5.95	99.72	6.78
Nadolol	104.32	8.69	98.72	4.43	98.82	2.48	95.50	5.70	104.85	16.13	105.16	9.59	102.77	6.15	91.91	4.49
Nicotinic acid	104.44	13.59	94.92	9.70	108.80	5.41	100.26	13.25	101.26	12.88	96.92	9.48	97.55	8.69	99.60	8.64
Olmesartan	118.42	17.36	109.70	9.60	105.76	13.66	108.50	6.11	109.29	14.26	101.71	10.30	98.26	13.28	97.63	10.57
Perindopril	107.62	19.75	115.00	5.18	114.12	13.57	114.00	3.72	100.09	16.48	112.55	9.16	107.55	9.45	111.73	6.62
Pindolol	98.28	14.65	101.82	6.41	103.04	8.73	86.38	4.30	109.19	17.40	104.23	10.24	99.57	6.80	86.43	3.24
Pitavastatin	117.84	18.58	105.30	9.47	112.48	8.72	109.16	9.64	103.21	17.75	94.78	12.47	100.48	8.54	93.23	6.90
Propranolol	101.68	8.22	110.86	12.11	94.46	13.23	85.44	5.82	110.76	8.99	111.38	11.18	100.39	12.07	87.25	9.16
Ramipril	112.74	18.58	106.56	8.36	92.82	9.22	90.24	7.04	106.27	13.47	108.06	11.57	99.47	6.45	97.21	6.61
Rosuvastatin	93.72	12.37	90.04	14.54	101.16	5.99	112.60	4.33	107.57	8.85	103.41	11.61	96.65	6.74	112.13	4.53
Spirono-lactone	110.14	13.57	111.52	6.69	93.36	10.21	93.98	7.81	109.89	12.02	106.97	5.64	97.33	10.36	93.37	7.69
Telmisartan	117.46	11.31	106.48	13.41	102.00	13.08	108.32	9.16	116.09	14.97	100.79	11.85	100.95	13.13	101.43	12.66
Terazosin	98.64	19.87	100.58	15.46	103.44	6.46	103.62	6.53	111.46	14.96	97.79	10.72	102.49	8.89	102.45	7.03
Triamterene	92.22	7.59	103.72	10.22	105.08	7.16	89.30	7.56	107.81	8.05	107.74	9.18	107.99	8.80	95.63	6.35
Warfarin	89.48	17.74	97.20	14.12	93.76	8.16	107.20	2.67	91.45	14.93	99.17	12.87	101.35	5.92	100.69	3.43

Table 6. Comparison with related literatures.

No	Drugs	LOQ concentration (ppb)	
		Developed method	References
1	Amlodipine	10	25[14]
2	Atenolol	20	10[14]
3	Atorvastatin	10	1[16]
4	Bendroflumethiazide	2	10[14]
5	Bisoprolol	2	25[14]
6	Diltiazem	1	25[14]
7	Doxazosin	5	10[14]
8	Enalapril	1	1[14]
9	Fluvastatin	20	1[16]
10	Furosemide	10	10[14]
11	HCTZ	100	10[14]
12	Indapamide	5	10[14]
13	Irbesartan	0.5	1[14]
14	Labetalol	10	1[14]
15	Lisinopril	10	1[14]
16	Losartan	2	1[14]
17	Lovastatin	10	2[16]
18	Metoprolol	0.5	25[14]
19	Mevastatin	5	5[16]
20	Moxonidine	5	10[14]
21	Perindopril	1	0.5[14]
22	Pitavastatin	0.5	1[16]
23	Ramipril	0.5	1[14]
24	Rosuvastatin	10	1[16]

Discussion

A quick, cost-effective, and specific "dilute-and-shoot" LC–MS/MS method with minimal sample preparation process was investigated and validated for the determination of 43 prescribed antihypertensive and related drugs in human urine. The optimal mass spectrometric and chromatographic parameters were investigated by applying experimental design approach. The validation results indicated that this screening LC-MS/MS method was specific, reproducible, and sensitive with the limit of detection from 0.1 to 50.0 μg/L. For now, this dilute-and-shoot LC–MS/MS method has simultaneously screened a largest number of hypertensive and related drugs in human urine. In comparison with other related literatures, of the 24 drugs compared, 11 were improved the sensitivity and 10 had higher concentration of detection (Table 6). The less sensitivity of these compounds could be due to the simultaneously screening a larger number of analytes in different structures. The assay could be optimized for concurrently analysis 43 drugs but difficult to obtain the best solution for each compound. In particular, 4 of 10 less sensitive drugs belong statin group, which has a more specialized dilute-and-shoot LC–MS/MS method developed by Jang et al. 2018.[16]

Future expansion of the assay could include the addition of drug metabolites, because some drugs have short half-life as well as are metabolised and excreted as metabolites in urine, such as spironolactone, aspirin, ramipril, or fluvastatin. The assay also could be applied to the analysis of actual urine samples to validate its clinical effectiveness in further experiments.

Conclusions

In conclusion, the developed method could be a promising approach for screening the presence of prescribed cardiovascular drugs in human urine.

Supporting Information

Supporting information is available at https://drive.google.com/file/d/1QHBrI7yTj0MhxCK1U-8tcBhLXTn__uGv/view?usp=sharing.

Acknowledgments

This research did not receive any specific grant from public, commercial, or non-profit funding agencies. The authors thank the Institute of New Drug Development Research and the Central Laboratory of Kangwon National University for the use of their analytical equipment.

References

1. World Health Organization. Cardiovascular diseases (CVDs), https://www.who.int/news-room/fact-sheets/detail/cardiovascular-diseases-(cvds)
2. Abegaz, T. M.; Shehab, A.; Gebreyohannes, E. A.; Akshaya, Bhagavathula, A. S.; Elnour, A. A. *Medicine* **2017,** 96, e5641, DOI: 10.1097/MD.0000000000005641.
3. Punt, A. M.; Stienstra, N. A.; van Kleef, M. E. A.; Lafeber, M.; Spiering, W.; Blankestijn, P. J.; Bots, M. L.; Maarseveen, E. M. V. *J. Chromatogr. B* **2019**, 1121, 103, DOI: 10.1016/j.jchromb.2019.05.013.
4. Richter, L. H. J.; Jacobs, C. M.; Mahfoud, F.; Kindermann, I.; Bohm, M.; Meyer, M. R. *Anal. Chim. Acta* **2019,** 1070, 69, DOI: 10.1016/j.aca.2019.04.026.
5. Dias, E.; Hachey, B.; McNaughton, C.; Nian, H.; Yu, C.; Straka, B.; Brown, N. J.; Caprioli, R. M. *J. Chromatogr. B* **2014,** 937, 44, DOI: 10.1016/j.jchromb.2013.08.010.
6. Tomaszewski, M.; White, C.; Patel, P.; Masca, N.; Damani, R.; Hepworth, J.; Samani, N. J.; Gupta, P.; Madira, W.; Stanley, A.; Williams, B. *Heart* **2014,** 100, 855, DOI: 10.1136/heartjnl-2013-305063.
7. Gonzalez, O.; Alonso, R. M.; Ferreirós, N.; Weinmann, W.; Zimmermann, R.; Dresen, S. *J. Chromatogr. B.* **2011,**

879, 243, DOI: 10.1016/j.jchromb.2010.12.007.
8. Murray, G. J.; Danaceau, J. P. *J. Chromatogr. B* **2009,** 877, 3857, DOI: 10.1016/j.jchromb.2009.09.036.
9. Guddat, S.; Solymos, E.; Orlovius, A.; Thomas, A.; Sigmund, G.; Geyer, H.; Thevis, M.; Schanzer, W. *Drug Test Anal.* **2011,** 3, 836, DOI: 10.1002/dta.372.
10. Sanchis, Y.; Coscollà, C.; Yusà, V. *Talanta* **2019,** 202, 42, DOI: 10.1016/j.talanta.2019.04.048.
11. Feng, S.; Enders, J. R.; Cummings, O. T.; Strickland, E. C.; McIntire, T.; McIntire, G. *J. Anal. Toxicol.* **2020**, 44, 331, DOI: 10.1093/jat/bkz098.
12. Cao, Z.; Kaleta, E.; Wang, P. *J. Anal. Toxicol.* **2015**, 39, 335, DOI: 10.1093/jat/bkv024.
13. Dahlin, J. L.; Palte, M. J.; LaMacchia, J.; Petrides, A. K. *The JALM*, **2019**, 3, 974, DOI: 10.1373/jalm.2018.027342.
14. Lawson, A. J.; Shipman, K. E.; George, S.; Dasgupta, I. *J. Anal. Toxicol.* **2016,** 40, 17, DOI: 10.1093/jat/bkv102.
15. Truong, Q. K., Mai X. L.; Lee, J. Y.; Rhee, J.; Vinh, D.; Hong, J.; Kim, K. H. *Arch. Pharm. Res.* **2018,** 41, 530, DOI: 10.1007/s12272-018-1011-9.
16. Jang, H.; Mai, X. L.; Lee, G.; Ahn, J. H.; Rhee, J.; Truong, Q. K.; Vinh, D.; Hong, J.; Kim, K. H. *Mass Spectrom. Lett.* **2018,** 9, 95, DOI: 10.5478/MSL.2018.9.4.95.
17. Sahu, P. K.; Ramisetti, N. R.; Cecchi, T.; Swain, S.; Patro, C. S.; Panda, J. *J. Pharm. Biomed. Anal.* **2018,** 147, 590, DOI: 10.1016/j.jpba.2017.05.006.

Vol. 12, No. 1, 2021
ISSN 2233-4203/ e-ISSN 2093-8950
ARTICLE www.msletters.org | Mass Spectrometry Letters

Determination of Nitarsone in Pork, Egg, Milk, Halibut, Shrimp, and Eel Using QuEChERS and LC-MRM

Jin Hee Kim[#], Yong Jin Jang[#], Dong Yoon Kim, Hyo Chun Lee, and Yong Seok Choi*

College of Pharmacy, Dankook University, Cheonan, Chungnam 31116, South Korea

Received February 12, 2021; Revised March 9, 2021; Accepted March 9, 2021
First published on the web March 31, 2021; DOI: 10.5478/MSL.2021.12.1.11

Abstract : Nitarsone is an organoarsenic antiprotozoal drug widely used to treat blackhead disease in turkeys and chickens. However, since its biological conversion into inorganic arsenic, a carcinogen was known, its residue in foods should be regulated. Thus, here, a novel method to determine residual nitarsone in various food commodities (pork, milk, egg, halibut, eel, and shrimp) using QuEChERS and LC-MRM was developed. The developed method was successfully validated through specificity, linearity (coefficient of determination, at least 0.991), recovery (R, 63.6 - 85.6%), precision (the relative standard deviation of R, 0.5 - 10.6%), and sensitivity (the lower limit of quantitation, 5 ppb) by following the Ministry of food and drug safety (MFDS) guidelines. The present method is the first mean to quantitate nitarsone using LC-MRM, and it was designed to be conveniently merged into a new method to quantitate multiple veterinary drugs for the positive list system (PLS). Therefore, the present method could contribute to fortify the food safety system in South Korea.

Keywords : nitarsone, food, QuEChERS, MRM, PLS

Introduction

Nitarsone (4-nitrophenylarsonic acid, Figure 1), an organoarsenic compound with antiprotozoal activity has been widely used to treat blackhead disease in turkeys and chickens.[1,2] In 2015, the US Food and Drug Administration (FDA) withdrew the approval for its applications in animal feed due to its biological conversion into inorganic arsenic, a carcinogen.[3] However, since it is still used in other countries, its regulation in various food commodities is needed.[4] Organoarsenic compounds including nitarsone are analyzed by inductively coupled plasma mass spectrometry (ICP-MS).[5,6] Additionally, HPLC-ultraviolet oxidation hydride generation-atomic fluorescence spectrometry (HPLC-UV-HG-AFS), HPLC-ultraviolet detector (HPLC-UV), and gas chromatography-mass spectrometry (GC–MS) were reported to be used to analyze nitarsone.[7-9] Among these techniques, ICP-MS is considered as the gold standard for nitarsone analysis due to its high sensitivity, but there are some drawbacks. First, ICP-MS is relatively less common in laboratories due to its cost.[10] Also, since ICP-MS analyzes targets in elemental ion forms, majority of veterinary drugs without rare element cannot be determined using ICP-MS.[11] It means that ICP-MS-based methods to determine nitarsone cannot be merged into a new method to analyze various kinds of veterinary drugs simultaneously.

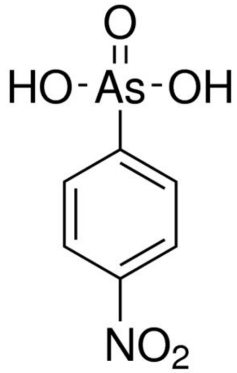

Figure 1. Chemical structure of nitarsone.

Thus, here, a novel method to determine residual nitarsone in various food commodities (pork, egg, milk, halibut, shrimp, and eel) using QuEChERS and LC-MRM was developed and validated. The present method is the first LC-MRM method to analyze nitarsone and could contribute to fortify the food safety system in South Korea.

[#]Both authors contributed equally to this work.
*Reprint requests to Yong Seok Choi
E-mail: analysc@dankook.ac.kr

Experimental

Chemicals and reagents

Nitarsone (analytical standard grade) was purchased from Santa Cruz Biotechnology (Dallas, TX, USA). Acetonitrile, methanol, and water were obtained from J. T. Baker (Phillipsburg, NJ, USA). Formic acid was purchased from Sigma-Aldrich (St. Louis, MO, USA). All solvents mentioned above were at least HPLC grade and used without further purification. All QuEChERS-related reagents were purchased from Phenomenex (Torrance, CA, USA).

Sample preparation

Samples (pork, egg, milk, halibut, shrimp, and eel) were obtained from local food markets and individual samples were homogenized (in the case of egg, blended without shell). A portion (2 g or 2 mL) of a homogenized sample was transferred to a 50-mL polypropylene (PP) conical tube and tubes were stored at -20°C until extraction and purification (E/P) processes. As the first step of E/P procedures, a frozen sample was thawed at room temperature. Then, the thawed sample was mixed with 0.2 mL of formic acid, 1 g of magnesium sulfate ($MgSO_4$), 0.25 g of sodium chloride (NaCl), 0.125 g of sodium citrate dibasic sesquihydrate (SCDS), 0.25 g of sodium citrate tribasic dihydrate (SCTD), and 10 mL of acetonitrile. The mixture was vortexed (for 10 min) and centrifuged (at 4°C and 2700 ×g for 10 min), and the whole top layer (organic layer) was transferred to a 15-mL PP conical tube containing 25 mg of primary secondary amine (PSA), 150 mg of $MgSO_4$, and 25 mg of C_{18}. The resulting mixture was vortexed (for 10 min) and centrifuged (at 4°C and 2700 ×g for 10 min), and the supernatant was completely taken for enrichment. After dried under nitrogen stream at 40°C, the residue was dissolved in 400 μL of a 50% aqueous methanol solution. Finally, the reconstituted solution was vortexed (for three min) and centrifuged (at 4°C and 2700 ×g for three min), and a portion of the supernatant was analyzed through liquid chromatography and tandem mass spectrometry (LC-MS/MS) (Figure 2). A matrix-matched standard (MMS) and a standard-spiked sample (SSS) were prepared by spiking an appropriate volume of a nitarsone standard solution into the final P/E extract from a blank matrix and into a blank matrix prior to P/E procedures, respectively.

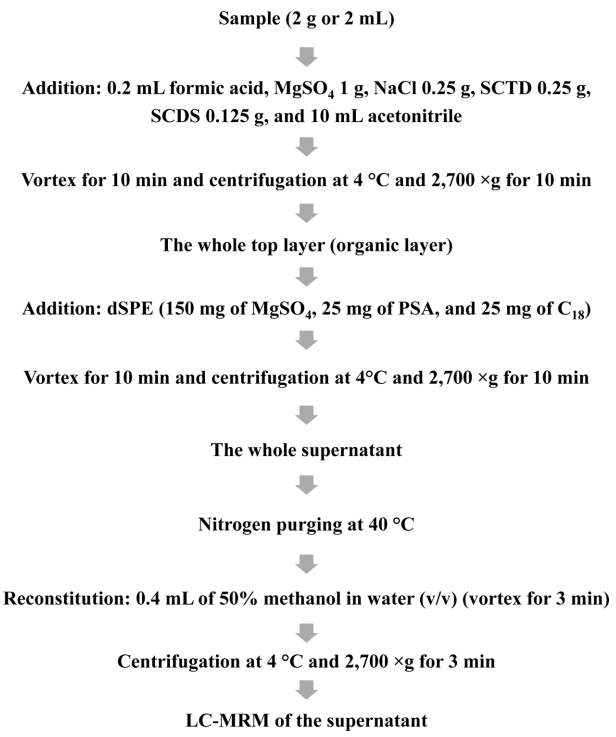

Figure 2. Schematic diagram of the present method using QuEChERS and LC-MRM.

LC-MS/MS

For separation and analysis of the P/E extract, a LC-MS/MS system composed of a Shimadzu Nexera UPLC system (Tokyo, Japan) and a Shimadzu LCMS 8050 triple quadrupole mass spectrometer were used. Additionally, electrospray ionization (ESI) with negative ion mode and a Phenomenex Luna C18 column (2.0 × 150 mm, 5 μm, Torrance, CA, USA) were employed. For separation, gradient mobile phase (MP) program between 0.1% (v/v) formic acid in water and 0.1% (v/v) formic acid in methanol at 0.25 mL/min for 14 minutes were used and the column was kept at 40°C (Table 1). In the case of the sample injector, its temperature and injection volume were 4°C and 10 μL, respectively. The sensitive determination of nitarsone through mass spectrometry was achieved by multiple reaction monitoring (MRM), a selective as well as sensitive MS/MS scan method. As shown in Table 2, three MRM transitions for nitarsone were prepared: the screening transition of 245.9 *m/z* (precursor ion) / 137.9 *m/z* (product ion) / -15 V (collision energy); the confirmatory transition 1 of 245.9 *m/z* / 107.8 *m/z* / -24 V; the confirmatory transition 2 of 245.9 *m/z* / 122.7 *m/z* / -27 V. Additional parameters for the mass spectrometer were as follows: nebulizing gas flow at 3 L/min, heating gas flow at 10 L/min, drying gas flow at 10 L/min, interface temperature at

Table 1. Gradient mobile phase program.

Time (minutes)	0.1% (*v*/*v*) Formic acid in water (%, *v*/*v*)	0.1% (*v*/*v*) Formic acid in methanol (%, *v*/*v*)
0.0	100.0	0.0
1.0	100.0	0.0
6.0	10.0	90.0
8.5	10.0	90.0
8.6	100.0	0.0
14.0	100.0	0.0

Table 2. Properties of nitarsone.

Compound	Molar mass (Da)	Retention time (minutes)	MRM transitions		
			Precusor ion (*m/z*)	[a]Product ion (*m/z*)	[b]CE (V)
Nitarsone	247.0	5.6	245.9 $[M-H]^-$	137.9	15
				107.8	24
				122.7	27

[a]The product ion of the screening transition; the product ion of a confirmatory transition
[b]Collision energy; the CE of the screening transition; the CE of a confirmatory transition

300°C, DL temperature at 250°C, and heating block temperature at 400°C. All data were acquired and analyzed using Lab Solutions (version 5.93, Shimadzu). For quantitation, peak area values of the screening transition from sample analyses were compared to calibration curves built using those from MMS analyses. However, a couple of preconditions were tested prior to quantitation. First, three transitions peaks should have the same retention time (the identity confirmation). Also, the signal-to-noise ratio (S/N) values of the screening transition peak and the confirmatory transition peaks should be at least 10 and at least 3, respectively (the sensitivity test).

Validation

The present method was validated in the aspects of specificity, linearity, recovery, precision, and sensitivity following guidelines of the ministry of food and drug safety, South Korea (MFDS).[12] First, the specificity was tested by comparisons between blank matrices and their conjugate SSSs (5 ppb). Also, linearity (the coefficient of determination, r^2) was evaluated by individual calibration curves built from analyses of 6 MMSs (5, 10, 20, 30, 40, and 50 ppb, $n = 3$). Third, a recovery (R) value was calculated by the division of the screening transition peak area of a SSS by that of its counter MMS. In each matrix, recovery values at three levels (5, 10, and 20 ppb) for three consecutive days were studied and computed ($n = 5$). In the case of precision, it was expressed by the relative standard deviation (RSD) of R values. Finally, the lower limit of quantitation (LLOQ), a parameter representing sensitivity was determined to the lowest concentration which satisfies R criteria of MFDS guidelines within the linear dynamic range.

Results and discussion

To develop a highly sensitive method to determine nitarsone in diverse kinds of food commodities, food matrices with broad spectrum of fat content (0.7, 0.9, 3.3, 7.4, 16.4 and 17.1% in shrimp, milk, halibut, egg, pork and eel, respectively), considered as a major interfering factor in food residual analyses, were cautiously selected as sample matrices.[13-15]

Since the merge of the present method to a novel PLS method to determine various veterinary drugs in foods in a near future was considered, there are a couple of unique points in the present method. First, no internal standard (IS) was employed in the present method, because IS is not used in multiresidual analysis methods. Also, MRM was carried out in negative ion mode, but the pH of MPs was set to 2.8. While there must have been a disadvantage in the aspect of sensitivity due to less deprotonation of nitarsone, LC conditions of present method became compatible to LC conditions of most residual veterinary drug analyses in foods. Consequently, regardless of these unique points, the present method was found to be good enough for quantitation with LLOQ of 5 ppb, the requirement for PLS.[16]

For MRM transitions, the $[M-H]^-$ ion (245.9 *m/z*) of nitarsone was selected as the precursor ion. Also, the ions with 137.9, 107.8 and 122.7 *m/z* values, the strongest, the second, and the third strongest fragment ions from the product ion scan of the $[M-H]^-$ ion of nitarsone, respectively, were decided as product ions (data not shown). Thus, the most sensitive 245.9/137.9 transition was used for quantitation (the screening transition), and other transitions (245.9/107.8 and 245.9/122.7 transitions) were used as confirmatory transitions to confirm the identities of ions detected (Table 2).

E/P of nitarsone in matrices were performed using QuEChERS in the present method. To obtain the best recovery, major steps (the amount of a sample, the composition of the extraction solvent, the volume of the extraction solvent, the composition of the dSPE adsorbent, and the amount of the dSPE adsorbent) of our previous QuEChERS-EDTA method were changed and their resulting recovery values were compared (data not shown).[14] As a result, a novel QuEChERS method optimized for E/P of nitarsone in various food commodities was confirmed (Figure 2).

The present method was validated in the aspects of specificity, linearity, R, precision, and sensitivity (Table 3). First, specificity was confirmed by the absence of the nitarsone screening transition peak at the retention time of nitarsone from a blank matrix (negative control) results (Figure 3). Second, since all calibration curves built by using MMSs (5-50 ppb) of individual matrices showed r^2 values of at least 0.991, its linearity satisfied MFDS

Table 3. Method validation results.

Matrices	Linearity ([a]r^2, 5-50 ppb)	Fortified concentration (ppb)	Intraday (n = 5)		Interday (n = 5, 3 days)		[c]LLOQ (ppb)
			Recovery (%)	[b]RSD (%)	Recovery (%)	[b]RSD (%)	
Pork	0.993	5	80.57	0.46	83.12	2.93	5
		10	79.97	4.50	80.56	3.11	
		20	85.56	1.57	83.35	2.88	
Egg	0.997	5	67.50	7.58	64.02	6.12	
		10	73.12	8.39	67.73	9.12	
		20	76.71	5.24	73.27	4.56	
Milk	0.991	5	69.74	4.23	63.59	10.56	
		10	71.70	8.85	75.35	5.93	
		20	75.90	8.42	73.54	5.27	
Halibut	0.999	5	81.20	1.65	81.58	4.43	
		10	79.05	3.37	78.62	2.72	
		20	83.17	2.54	78.29	5.75	
Shrimp	0.995	5	68.27	2.84	70.25	4.34	
		10	65.88	3.95	68.02	6.08	
		20	76.99	2.97	73.95	3.53	
Eel	0.991	5	71.66	5.33	72.39	7.34	
		10	73.70	1.52	73.62	3.35	
		20	73.95	3.27	74.41	4.77	

[a]Coefficient of determination
[b]Relative standard deviation of recovery
[c]Lower limit of quantitation

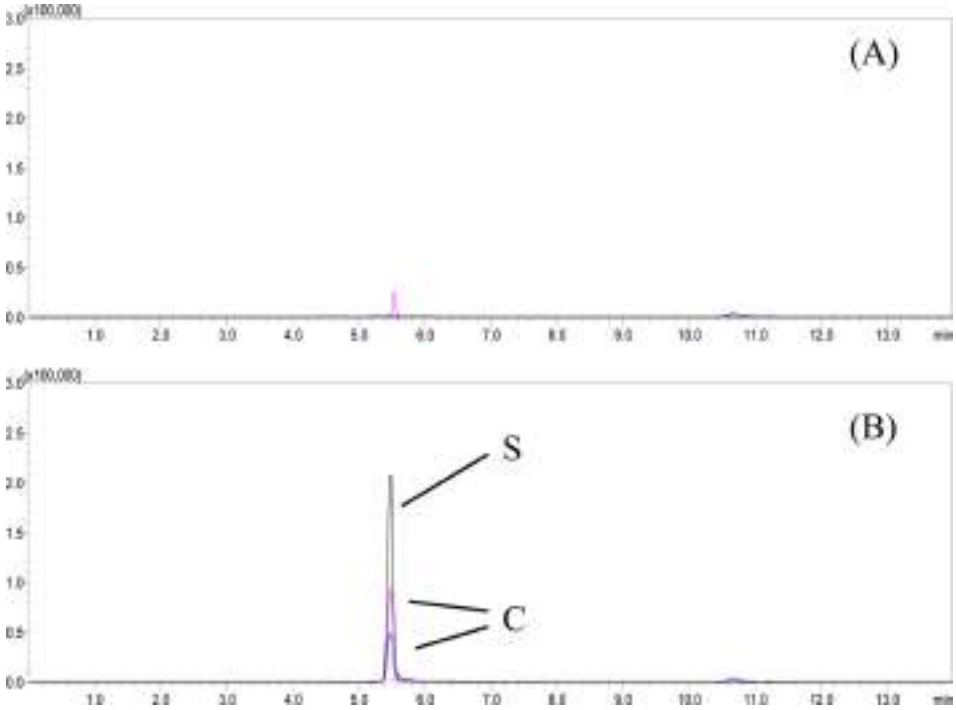

Figure 3. MRM chromatograms from blank halibut (A) and standard (5 ppb)-spiked halibut (B) analyses. S and C stand for the screening transition peak and the confirmatory transition peaks, respectively.

guidelines (at least 0.98).[12] Third, R values evaluated between 5 and 20 ppb were 63.6-85.6% with intra-day RSD less than 8.9% and inter-day RSD less than 10.6% and they are good enough to pass the criteria of MFDS guidelines.[12] Finally, the S/N values of all nitarsone MRM peaks observed over validation studies were found to be higher than 10 (for screening transition) and 3 (for confirmatory transitions) (data not shown). Thus, the good quantitative performance (including LLOQ of 5 ppb) of the present method was proved and it is good enough to be used for the PLS which requires LLOQ of 5 ppb.[16]

The validated method was applied to determine residual nitarsone in pork, milk, egg, halibut, eel, and shrimp (three samples per commodity) purchased from local food markets. Each sample extract was prepared and analyzed in triplicates and there was no sign of nitarsone residue in all samples (data not shown).

Conclusions

As a part of efforts to establish the PLS in South Korea, a novel method to determine residual nitarsone in various food commodities (pork, milk, egg, halibut, eel, and shrimp) using QuEChERS and LC-MRM was developed and validated. This is the first method to quantitate nitarsone using LC-MRM. Also, the present method was designed to be conveniently merged into a new method to quantitate multiple veterinary drugs for PLS. Therefore, the present method could contribute to fortify the food safety system in South Korea.

Acknowledgements

This research was supported by a grant (16162MFDS582) from Ministry of Food and Drug Safety, Republic of Korea in 2016-2018. Also, this work was funded by the Research-Focused Department Promotion Project as a part of the University Innovation Support Program 2020 to Dankook University. The authors would like to thank Dr. Sang Beom Han (Chung-Ang University), and Dr. Ho-Chul Shin (Konkuk University) for their technical support.

References

1. Cui, J; Xiao, Y; Dai, L; Zhao, X; Wang, Y. *Food Anal. Methods* **2013**, 6, 370, DOI: 10.1007/s12161-012-9533-0.
2. Eom, H. Y.; Yang, D. H.; Suh, J. H.; Kim, U. Y.; Kim, J. H.; Cho, H. D.; Han, S. B. *J. Chromatogr. B* **2015**, 1006, 151, DOI: http://dx.doi.org/10.1016/j.jchromb.2015.10.034.
3. Nachman, K. E.; Love, D. E.; Baron, P. A.; Nigra, A. E.; Murko, M.; Raber, G.; Francesconi, K. A.; Bavas-acien, A. *Environ. Health Perspect.* **2017**, 125, 363, DOI: 10.1289/EHP225.
4. Liu, D. F.; Huang, X. N.; Cheng, R. F.; Min, D.; Cheng, L.; Zhao, F.; Chen, J. J. *ACS EST Water*, *accepted*, DOI: https://doi.org/10.1021/acsestwater.0c00124.
5. Liu, L.; He, B.; Yun, Z.; Sun, J.; Jiang, G. *J. Chromatogr. A* **2013**, 1304, 227, DOI: 10.1016/j.chroma.2013.07.034.
6. Reid, M. S.; Hoy K. S.; Schofield, J. R. M.; Uppal, J. S.; Lin, Y.; Lu, X.; Peng, H.; Chris Le, X. *Trends Anal. Chem.* **2020**, 123, 115770, DOI: https://doi.org/10.1016/j.trac.2019.115770.
7. Sánchez-Rodas, D.; Gómez-Ariza, J. L.; Oliveira, V. *Anal. Bioanal. Chem.* **2006**, 385, 1172, DOI: 10.1007/s00216-006-0379-4.
8. Czaplickaa, M.; Jaworekb, K.; Klytaa, J. *Desalin. Water Treat.* **2019**, 172, 386, DOI: 10.5004/dwt.2019.24610.
9. Chen, D.; Zhang, H.; Tao, Y.; Wang, Y.; Huang, L.; Liu, Z.; Pan, Y.; Peng, D.; Wang, X.; Dai, M.; Yuan, Z. *J. Chromatogr. B* **2011**, 879, 716, DOI: 10.1016/j.jchromb.2011.02.013.
10. Wilschefski, S. C.; Baxter, M. R. *Clin. Biochem. Rev.* **2019**, 40, 115, DOI: 10.33176/AACB-19-00024.
11. Telgmann, L.; Lindner, U.; Lingott, J.; Jakubowski, N. *Phys. Sci. Rev.* **2016**, 1, 20160064, DOI: https://doi.org/10.1515/psr-2016-0058.
12. Ministry of food and drug safety, South Korea, Guidelines for analytical method validation.; See https://www.mfds.go.kr/brd/m_210/view.do?seq=12920&srchFr=&srchTo=&srchWord=%ED%99%94%EC%9E%A5%ED%92%88&srchTp=0&itm_seq_1=0&itm_seq_2=0&multi_itm_seq=0&company_cd=&company_nm=&page=2.
13. Ministry of food and drug safety, South Korea. Food and nutrient data system.; See https://www.foodsafetykorea.go.kr/portal/healthyfoodlife/foodnutrient/simpleSearch.do?menu_grp=MENU_NEW03&menu_no=2805.
14. Cho, H. R.; Park, J. S.; Kim, J. H.; Han, S. B.; Choi, Y. S. *Anal. Bioanal. Chem.* **2015**, 407, 9043, DOI: 10.1007/s00216-015-9071-x.
15. Cho, H. R.; Kim, D. Y.; Lee, H. C.; Han, S. B.; Shin, H. C.; Choi, Y. S. *Mass Spectrom. Lett.* **2018**, 4, 100, DOI: 10.5478/MSL.2018.9.4.100.
16. Ministry of food and drug safety, South Korea. PLS on veterinary drugs.; See https://mfds.go.kr/brd/m_209/view.do?seq=43393.

Vol. 12, No. 1, 2021
ISSN 2233-4203/ e-ISSN 2093-8950
ARTICLE www.msletters.org | Mass Spectrometry Letters

Correlation between the Content and Pharmacokinetics of Ginsenosides from Four Different Preparation of Panax Ginseng C.A. Meyer in Rats

Ji-Hyeon Jeon[1], Jaehyeok Lee[1], Chul Haeng Lee[2], Min-Koo Choi[2]*, and Im-Sook Song[1]*

[1]BK21 FOUR Community-Based Intelligent Novel Drug Discovery Education Unit, Vessel-Organ Interaction Research Center (VOICE), Research Institute of Pharmaceutical Sciences, College of Pharmacy, Kyungpook National University, Daegu, 41566, Korea
[2]College of Pharmacy, Dankook University, Cheon-an, 31116, Korea

Received Feburary 25, 2021; Revised March 17, 2021; Accepted March 22, 2021
First published on the web March 31, 2021; DOI: 10.5478/MSL.2021.12.1.16

Abstract : We aimed to compare the content of ginsenosides and the pharmacokinetics after the oral administration of four different ginseng products at a dose of 1 g/kg in rats. The four different ginseng products were fresh ginseng extract, red ginseng extract, white ginseng extract, and saponin enriched white ginseng extract prepared from the radix of Panax ginseng C.A. Meyer. The ginsenoside concentrations in the ginseng product and the rat plasma samples were determined using a liquid chromatography-tandem mass spectrometry (LC-MS/MS). Eight or nine ginsenosides of the 15 tested ginsenosides were detected; however, the content and total ginsenosides varied depending on the preparation method. Moreover, the content of triglycosylated ginsenosides was higher than that of diglycosylated ginsenosides, and deglycosylated ginsenosides were not present in any preparation. After the single oral administrations of four different ginseng products in rats, only four ginsenosides, such as 20(S)-ginsenosides Rb1 (GRb1), GRb2, GRc, and GRd, were detected in the rat plasma samples among the 15 ginsenosides tested. The plasma concentrations of GRb1, GRb2, GRc, and GRd were different depends on the preparation method but pharmacokinetic features of the four ginseng products were similar. In conclusion, a good correlation between the area under the concentration curve and the content of GRb1, GRb2, and GRc, but not GRd, in the ginseng products was identified and it might be the result of their higher content and intestinal biotransformation of the ginseng product.

Keywords : ginseng product preparation, LC-MS/MS, ginsenoside content, pharmacokinetics

Introduction

Ginseng, Panax ginseng C.A. Meyer (Araliaceae), has been one of the most popular herbal medicines in the world for > 2000 years; it is especially popular in East Asian countries, including Korea, China, and Japan.[1,2] Ginsenosides, also called steroid-like saponins, are considered as the major active pharmacological constituents of ginseng.[1,3] Ginseng and its associated ginsenosides are reported to exert antineoplastic, antihypertensive, antidiabetic, anti-inflammatory, antioxidative, anti-allergic, neuroprotective, hepatoprotective, and immunologic effects.[3-6] In addition to their therapeutic effects, ginseng products are frequently administered as health supplements with therapeutic drugs, such as anticancer drugs and anti-diabetes drugs, and for fatigue and physical performance.[7]

Therefore, the market for ginseng products has rapidly grown, and ginseng products include fresh ginseng, white ginseng product, and red ginseng extracts and others. These ginseng products are processed via steaming, drying, extraction with water or ethanol, and concentration and these processes lead to biochemical transformations in the constituent peptides, ginsenosides, polysaccharides, fatty acids, and polyacetylenic alcohols.[8] Thus, the content of ginsenosides may vary during these processes.

Therefore, we aimed to analyze the content of ginsenosides in the ginseng products prepared from different process and to investigate the pharmacokinetics of ginsenosides after oral administration of these ginseng products to rats at a dose of 1 g/kg.

Experimental

Chemicals and reagents

Ginseng products were obtained from Punggi Ginseng Cooperative Association (Youngjoo, Kyungpook, Korea).

*Reprint requests to Min-Koo Choi, and Im-Sook Song
E-mail: minkoochoi@dankook.ac.kr and isssong@knu.ac.kr

The preparation scheme for the four different ginseng products, including fresh ginseng extract, red ginseng extract, white ginseng extract, and saponin enriched white ginseng extract are shown in Figure 1. 20(S)-ginsenosides Rb1 (GRb1), GRb2, GRc, GRd, GRg1, GRg3, GRe, GRh1, GF1, GF2, 20(S)-compound K (CK), 20(S)-proptopanaxadiol (PPD), and 20(S)-protopanaxatriol (PPT) were purchased from the Ambo Institute (Daejeon, Korea). Berberine and ^{13}C-caffeine were used as internal standards (IS) and were purchased from Sigma–Aldrich Chemical Co. (St. Louis, MO, USA). All the other chemicals and solvents were of reagent or analytical grade.

Pharmacokinetic study

All animal procedures were approved by the Animal Care and Use Committee of Kyungpook National University (Approval No. KNU 2018-0077 and KNU 2019-0005) and carried out in accordance with the National Institutes of Health guidelines for the care and use of laboratory animals.

The male Sprague Dawley rats (7–8 week old, weighing 225–270 g) were purchased from the Samtako (Osan, Kyungi-do, Korea). After their arrival, the rats were housed with a 12 h light/dark cycle; food and water were supplied ad libitum for 1 wk. The rats were made to fast for 16 h; however, free access to water was given before the pharmacokinetic experiments. Four ginseng products (Figure 1) were suspended with distilled water (1 g/kg/ 2 mL) and administered to the rats using oral gavage at a dose of 1 g/kg. Blood samples were withdrawn from the cannulated femoral artery at 0.25, 0.5, 1, 2, 4, 8, and 24 h after the administration of ginseng products. Blood samples were centrifuged at 16000 rpm for 1 min, and aliquots (30 μL) of plasma samples were stored at -80°C until the analysis of ginsenosides.

LC-MS/MS analysis of ginsenosides

The concentrations of ginsenosides were analyzed using a modified liquid chromatography-tandem mass spectrometry (LC-MS/MS) method[9-11] using an Agilent 6470 triple quadrupole LC-MS/MS system (Agilent, Wilmington, DE, USA). In order to analyze GRb1, GRb2, GRc, GRd, GRe, GRf, GRg1, GRg3, GF1, and GF2, 200 μL of an IS (0.05 ng/mL berberine in methanol) was added to 30 μL of plasma samples. Thereafter, the mixture was vortexed for 15 min and centrifuged at 16,000 × g for 5 min. After centrifugation, 200 μL of the supernatant was transferred to a clean tube and evaporated to dryness under nitrogen stream at 40°C. The residue was reconstituted using 100 μL of 70% methanol supplemented with 0.1% formic acid, and a 10 μL aliquot was injected into the LC-MS/MS system. The ginsenosides were separated on a Polar RP column (150 × 2.0 mm, 4.0 μm particle size) with mobile phase comprising 0.1% formic acid in water (phase A) and 0.1% formic acid in methanol (phase B) at a flow rate of 0.27 mL/min. The gradient elution was used: 69% of phase B for 0–2.0 min, 69%–85% of phase B for 2.0–4.0 min, 85%–69% of phase B for 6.0–6.5 min.

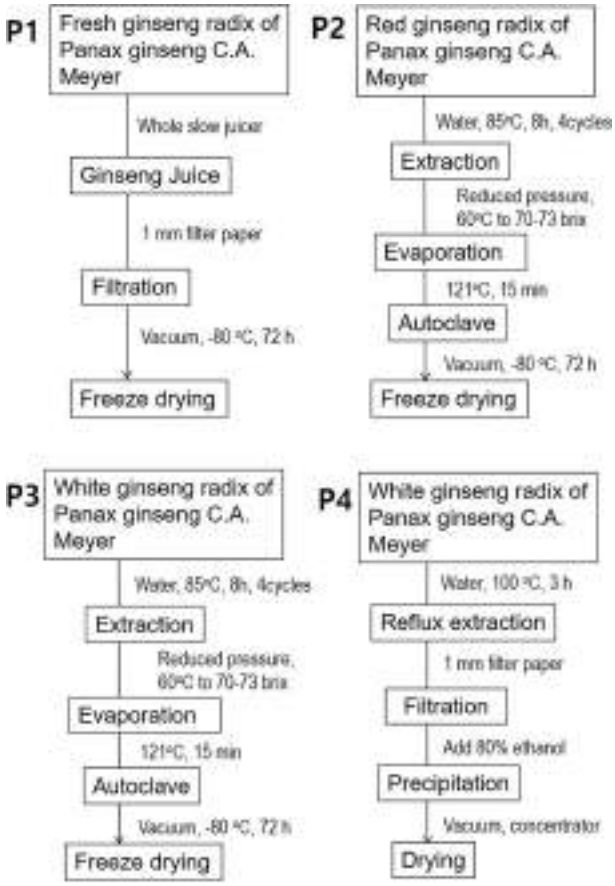

Figure 1. The preparation scheme for four different ginseng products prepared from the radix of Panax ginseng C.A. Meyer. P1, fresh ginseng extract; P2, red ginseng extract; P3, white ginseng extract; P4, saponin enriched white ginseng extract.

To analyze GRh1, GRh2, CK, PPD, and PPT, 30 μL of an IS (20 ng/mL 13C-caffeine in water) and 400 μL of methyl tert-butyl ether was added to 30 μL of plasma samples. The mixture was vortexed for 10 min and then centrifuged at 16,000 × g for 5 min. After centrifugation, the samples were frozen at -80°C for 4 h. Next, the upper layer was transferred to a clean tube and evaporated to dryness under a nitrogen stream. The residue was reconstituted with 100 μL of 80% methanol supplemented with 0.1% formic acid, and a 10-μL aliquot was injected into the LC-MS/MS system. Ginsenosides were separated on a Luna C18 column (150 × 2.0 mm, 3.0 μm particle size) with mobile phase consisting of 0.1% formic acid in water (8%) and 0.1% formic acid in methanol (92%) at a flow rate of 0.15 mL/min.

The ginsenoside content in the RGE was quantified in a similar manner. The ginseng product (100 mg) was diluted

Table 1. MS/MS parameters for the detection of the ginsenosides and IS prepared from protein precipitation and liquid-liquid extraction method.

Ginsenosides	Precursor ion	Product ion	Retention time (min)	Collision energy
Protein precipitation method				
GRb1	1131.6	365.1	4.6	65
GRc/GRb2	1101.6	335.1	4.7/5.5	60
GRd	969.9	789.5	6.6	50
GRe	969.9	789.5	2.0	50
GRf	823.5	365.1	3.2	55
GRg1	824.0	643.6	2.1	40
GRg3	807.5	365.1	9.3	60
GF1	661.5	203.1	4.5	40
GF2	807.5	627.5	9.3	40
Berberine (IS)	336.1	320.0	4.5	30
Liquid-liquid extraction method				
GRh1	603.4	423.4	3.1	10
GRh2	587.4	407.4	7.1	15
CK	645.5	203.1	6.3	35
PPD	425.3	109.1	10.9	25
PPT	441.3	109.1	3.9	30
^{13}C-caffeine (IS)	198.0	140.0	2.9	20

100-fold with 80% methanol, and 30 μL of the diluted sample was prepared using the method described previously. Aliquots (10 μL) of the supernatant were directly injected into the LC-MS/MS system.

Quantification was performed using multiple reaction monitoring in positive ion mode, and the details are shown in Table 1. The standard calibration curve for the mixture of 15 ginsenosides was linear in the concentration range of 0.5–200 ng/mL for the plasma samples, and the inter-day and intra-day precision and accuracy for ginsenosides was < 15%.

Data Analysis

The pharmacokinetic parameters were determined with non-compartmental analysis (WinNonlin® 2.0; Pharsight, Mountain View, CA, USA).[6] All data are expressed as mean ± standard deviation values.

Results and Discussion

Ginsenosides content in four ginseng product

The ginseng product prepared from the radix of *Panax ginseng* C.A. Meyer contained eight or nine ginsenosides of the 15 tested ginsenosides (Table 2). The ginsenoside content varies as per the preparation method of ginseng product, such as steaming, extraction, and drying; each affect the composition of the final ginseng product.[12] In red ginseng extract and white ginseng, the sum of PPD-type ginsenosides was higher that the sum of PPT-type ginsenosides, consistent with that in previous reports.[7,13] However, the fresh ginseng and saponon enriched white ginseng extract showed a higher sum of PPT-type ginsenosides than that of PPD-type. The results suggested that steaming and extraction with water may increase the content of PPD-type ginsenosides. Among them, triglycosylated ginsenosides, such as GRb1, GRb2, GRc, and GRd were present in the highest content compared with the diglycosylated ginsenosides. Likewise, triglycosylated PPT-type ginsenosides, such as GRe and GRg1, showed higher content than diglycosylated ginsenosides. In all ginseng products, mono-glycosylated or deglycosylated ginsenosides that need enzymatic deglycosylation from tri- or diglycosylates were not detected (Table 2).[7]

Table 2. Content of ginsenosides in the four ginseng products.

		Ginsenoside content (mg/g extract)			
		P1	P2	P3	P4
PPD-type	GRb1	1.4 ± 0.1	2.4 ±0.2	5.7 ± 0.04	1.6 ± 0.0
	GRb2	0.7 ± 0.02	1.6 ± 0.06	3.7 ± 0.06	0.5 ± 0.0
	GRc	0.5 ± 0.01	1.1 ± 0.04	2.7 ± 0.06	0.4 ± 0.0
	GRd	0.1 ± 0.0	0.7 ± 0.02	0.9 ± 0.05	0.07 ± 0.0
	GRh2	ND	ND	ND	ND
	GRg3	0.1 ± 0.0	1.2 ± 0.02	0.9 ± 0.01	0.2 ± 0.0
	GF2	ND	ND	ND	ND
	CK	ND	ND	ND	ND
	PPD	ND	ND	ND	ND
	Sum	2.7	8.2	13.9	2.8
PPT-type	GRe	1.5 ± 0.07	1.8 ± 0.06	2.8 ± 0.05	0.6 ± 0.2
	GRf	0.3 ± 0.0	0.8 ± 0.02	0.8 ± 0.01	ND
	GRh1	ND	0.9 ± 0.03	0.2 ± 0.0	0.9 ± 0.08
	GRg1	1.7 ± 0.09	1.6 ± 0.01	3.7 ± 0.07	4.7 ± 0.5
	GF1	ND	ND	ND	ND
	PPT	ND	ND	ND	ND
	Sum	3.6	5.1	7.5	6.2

P1, Fresh ginseng extract; P2, Red ginseng extract; P3, White ginseng extract; P4, Saponin enriched white ginseng extract; ND, not detected

Data represents the mean ± standard deviation (n = 3).

Plasma concentrations of ginsenosides in rats

The plasma concentrations of ginsenosides after oral administration of four ginseng products in rats are shown in Figure 2, and the relevant pharmacokinetic parameters are presented in Table 3. After the single oral administration of the four different ginseng product in rats, only four ginsenosides were detected in the rat plasma samples among the 15 ginsenosides that were tested, which is consistent with the human case.[10] As shown in Figure 2,

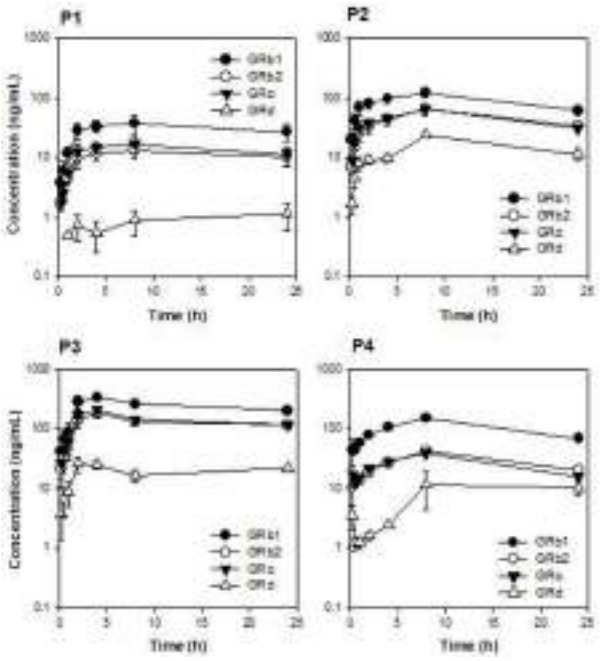

Figure 2. Plasma concentration-time profile of the ginsenoside GRb1, GRb2, GRc, and GRd after an oral administration of four ginseng products (1 g/kg) in rats. P1, Fresh ginseng extract; P2, Red ginseng extract; P3, White ginseng extract; P4, Saponin enriched white ginseng extract. Each data point represents the mean ± standard deviation (n = 4).

Table 3. Pharmacokinetic parameters of ginsenoside GRb1, GRb2, GRc, and GRd in rats.

		T_{max} (h)	C_{max} (ng/mL)	AUC (ng·h/mL)	MRT (h)
P1	GRb1	5.6 ± 1.0	39.2 ± 12	751.6 ± 236	11.6 ± 0.1
	GRb2	7.2 ± 0.8	13.3 ± 3.6	271.6 ± 75.7	11.8 ± 0.2
	GRc	6.4 ± 1.0	17.7 ± 5.1	335.5 ± 103	11.2 ± 0.3
	GRd	17 ± 3.9	1.3 ± 0.5	19.93 ± 10.0	13.9 ± 1.7
P2	GRb1	8.0 ± 0.0	123 ± 19	2223 ± 319	10.6 ± 0.2
	GRb2	8.0 ± 0.0	66.7 ± 16	1152 ± 249	11.1 ± 0.3
	GRc	8.0 ± 0.0	65.2 ± 9.3	1137 ± 132	10.7 ± 0.3
	GRd	8.0 ± 0.0	24.6 ± 2.6	389.6 ± 45.7	11.0 ± 0.5
P3	GRb1	2.6 ± 0.6	360 ± 54	5839 ± 577	11.3 ± 0.5
	GRb2	3.4 ± 0.6	189 ± 26	3082 ± 315	11.8 ± 0.5
	GRc	2.6 ± 0.6	221 ± 32	3360 ± 351	11.3 ± 0.4
	GRd	3.0 ± 0.5	34.5 ± 4.7	470.1 ± 34.9	12.9 ± 0.9
P4	GRb1	6.4 ± 1.5	162 ± 14	2619 ± 205	10.4 ± 0.1
	GRb2	6.4 ± 1.5	45.8 ± 5.5	725.8 ± 80.9	10.8 ± 0.2
	GRc	6.4 ± 1.5	47.2 ± 5.3	666.9 ± 47.2	10.0 ± 0.2
	GRd	13 ± 4.7	17.8 ± 6.1	212.5 ± 62.7	15.6± 2.1

P1, Fresh ginseng extract; P2, Red ginseng extract; P3, White ginseng extract; P4, Saponin enriched white ginseng extract; C_{max}: maximum plasma concentration; T_{max}: time to reach C_{max} ; AUC: area under the plasma concentration-time curve; MRT: mean residence time.
Data expressed as mean± standard deviation (n = 4).

GRb1, GRb2, GRc, and GRd in rat plasma were all found in the four ginseng products, and their plasma concentration profiles in rats were similar. That is, GRb1 had the highest concentration and GRd had the lowest concentration. Moreover, the plasma concetration of these four ginsenosides were maintained stably for 24 h, limiting the calculation of elimination half-life.

However, other PPD-type ginsenosides were not detected in the rat plasma samples after single administration of the ginseng product. In other studies after repeated oral administration of red ginseng extract, GRg3, CK, and PPD were detected in mice, rats, and humans.[9-11] Although the content of PPT-type ginsenosides was comparable or lower than that of PPD-type ginsenosides, none of the PPT-type ginsenosides were detected in the rat plasma samples in this study. With repeated oral administration of red ginseng extract, only GRe was detected in mice, and PPT was detected in rats and humans.[9,11] This could be attributed to the limited intestinal absorption or faster metabolism and elimination of PPT-type ginsenosides than in PPD-type ginsenosides.[11,14]

Then, we compared the plasma concentrations of GRb1, GRb2, GRc, and GRd with their content in ginseng products. Correlation analyses on the pharmacokinetic parameters of GRb1, GRb2, GRc, and GRd revealed a

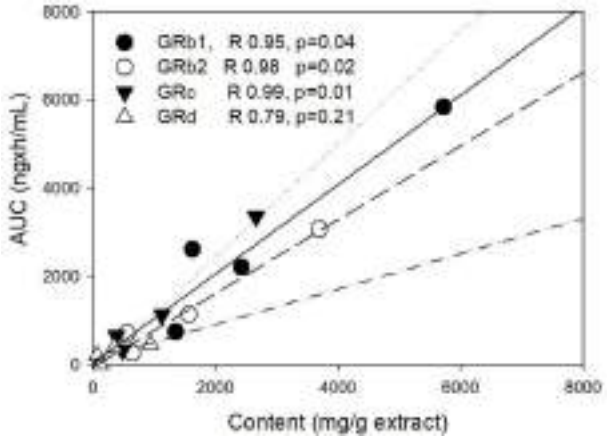

Figure 3. Correlation between the ginsenoside content and the area under the plasma concentration curve (AUC) of ginsenosides after oral administration of four ginseng products (1 g/kg) in rats. The data are taken from Table 2 and 3.

good correlation between the AUC values and the content of GRb1, GRb2, and GRc, but not GRd in ginseng product (Figure 3). In our previous results, the fecal recovery of

GRb1, GRb2, and GRc was < 10% of the oral intake; however, GRd was ~291% of the oral intake.[11] It suggested that GRb1, GRb2, and GRc were transformed into GRd; thus, the plasma concentrations of GRd could be higher than the content of GRd in the ginseng product. The results suggested that the pharmacokinetic properties of various ginsenosides, including GRb1, GRb2, GRc, and GRd could be determined by the composition of ginseng product as well as the intestinal biotransformation of ginsenosides. Therefore, researchers should be careful when selecting the ginseng product to explore the pharmacology and therapeutic effect of ginseng with a specific focus on the individual ginsenosides.

Conclusions

In this study, we investigated and compared the content of individual ginsenosides from four different ginseng products prepared from the radix of Panax ginseng C.A. Meyer with the pharmacokinetics after oral administration of these products. The major ginsenosides found in the plasma were GRb1, GRb2, GRc, and GRd, which are present in the highest content in ginseng products. Consequently, the good correlation between the AUC values and the content of GRb1, GRb2, and GRc, but not GRd, in the ginseng product might be the result of their higher concentration in the ginseng product and intestinal biotransformation process from GRb1, GRb2, and GRc to GRd. A strategy to increase the ginsenoside content of interest in the ginseng product or to modulate the metabolic biotransformation may improve the plasma ginsenoside concentrations and therapeutic response of the ginseng product.

Acknowledgments

This work was supported by the National Research Foundation of Korea (NRF) grant funded by the Korea government (MSIT) (No. NRF-2020R1I1A3074384 and NRF-2020R1A5A2017323).

References

1. Ru, W.; Wang, D.; Xu, Y.; He, X.; Sun, Y.E.; Qian, L.; Zhou, X.; Qin, Y. *Drug Discov. Ther.* **2015**, 9, 23, DOI: 10.5582/ddt.2015.01004.
2. Lee, C. H.; Kim, J. H. *J. Ginseng Res.* **2014**, 38, 161, DOI: 10.1016/j.jgr.2014.03.001.
3. Kim, J. H.; Yi, Y. S.; Kim, M. Y.; Cho, J. Y. *J. Ginseng Res.* **2017**, 41, 435, DOI: 10.1016/j.jgr.2016.08.004.
4. Yun, T. K.; Choi, S. Y.; Yun, H. Y. *J. Korean Med. Sci.* **2001**, 16, S19, DOI: 10.3346/jkms.2001.16.S.S19.
5. Gui, Q. F.; Xu, Z. R.; Xu, K. Y.; Yang, Y. M. *Medicine* **2016**, 95, e2584, DOI: 10.1097/MD.0000000000002584.
6. Park, T. Y.; Hong, M.; Sung, H.; Kim, S.; Suk, K. T. *J. Ginseng Res.* **2017**, 41, 450, DOI: 10.1016/j.jgr.2016.11.004.
7. Choi, M. K.; Song, I. S. *Arch. Pharm. Res.* **2019**, 42, 862, DOI: 10.1007/s12272-019-01184-3.
8. Lee, S. M.; Bae, B. S.; Park, H. W.; Ahn, N. G.; Cho, B. G.; Cho, Y. L.; Kwak, Y. S. *J. Ginseng Res.* **2015**, 39, 384, DOI: 10.1016/j.jgr.2015.04.009.
9. Jin, S.; Jeon, J. H.; Lee, S.; Kang, W. Y.; Seong, S. J.; Yoon, Y. R.; Choi, M. K.; Song, I. S. *Molecules* **2019**, 24, 2618, DOI: 10.3390/molecules24142618.
10. Choi, M. K.; Jin, S.; Jeon, J. H.; Kang, W. Y.; Seong, S. J.; Yoon, Y. R.; Han, Y. H.; Song, I. S. *J. Ginseng Res.* **2020**, 44, 229, DOI: 10.1016/j.jgr.2018.10.006.
11. Jeon, J. H.; Lee, J.; Choi, M. K.; Song, I. S. *Arch. Pharm. Res.* **2020**, 43, 1335, DOI: 10.1007/s12272-020-01289-0.
12. Choi, I. D.; Ryu, J. H.; Lee, D. E.; Lee, M. H.; Shim, J. J.; Ahn, Y. T.; Sim, J. H.; Huh, C. S.; Shim, W. S.; Yim, S. V.; Chung, E. K.; Lee, K. T. *Evid.-Based Complement Alternat. Med.* **2016**, 2016, 3908142, DOI: 10.1155/2016/3908142.
13. Chen, C. F.; Chiou, W. F.; Zhang, J. T. *Acta Pharmacol. Sin.* **2008**, 29, 1103, DOI: 10.1111/j.1745-7254.2008.00868.x.
14. Jiang, R.; Dong, J.; Li, X.; Du, F.; Jia, W.; Xu, F.; Wang, F.; Yang, J.; Niu, W.; Li, C. *Br. J. Pharmacol.* **2015**, 172, 1059, DOI: 10.1111/bph.12971.

Vol. 12, No. 1, 2021
ISSN 2233-4203/ e-ISSN 2093-8950
ARTICLE www.msletters.org | Mass Spectrometry Letters

Liquid Chromatography-Tandem Mass Spectrometric Analysis of Nannozinone A and Its Application to Pharmacokinetic Study in Mice

Chul Haeng Lee[1#], Soobin Kim[1#], Jaehyeok Lee[2], Ji-Hyeon Jeon[2], Im-Sook Song[2], Young Taek Han[1]*, and Min-Koo Choi[1]*

[1]*College of Pharmacy, Dankook University, Cheon-an, 31116, Korea*
[2]*College of Pharmacy and Research Institute of Pharmaceutical Sciences, Kyungpook National University, Daegu, 41566, Korea*

Received February 7, 2021, Revised March 16, 2021, Accepted March 25, 2021
First published on the web March 31, 2021; DOI: 10.5478/MSL.2021.12.1.000

Abstract : We aimed to develop and validate a sensitive analytical method of nannozinone A, active metabolite of Nannochelins A extracted from the Myxobacterium Nannocytis pusilla, in mouse plasma using a liquid chromatography-tandem mass spectrometry (LC-MS/MS). Mouse plasma samples containing nannozinone A and ^{13}C-caffeine (internal standard) were extracted using a liquid-liquid extraction (LLE) method with methyl *tert*-butyl ether. Standard calibration curves were linear in the concentration range of 1 - 1000 ng/mL ($r^2 > 0.998$) with the inter- and intra-day accuracy and precision results less than 15%. LLE method gave results in the high and reproducible extraction recovery in the range of 78.00–81.08% with limited matrix effect in the range of 70.56-96.49%. The pharmacokinetics of nannozinone A after intravenous injection (5 mg/kg) and oral administration (30 mg/kg) of nannozinone A were investigated using the validated LC-MS/MS analysis of nannozinone A. The absolute oral bioavailability of nannozinone A was 8.82%. Plasma concentration of nannozinone A after the intravenous injection sharply decreased for 4 h but plasma concentration of orally administered nannozinone A showed fast distribution and slow elimination for 24 h. In conclusion, we successfully applied this newly developed sensitive LC-MS/MS analytical method of nannozinone A to the pharmacokinetic evaluation of this compound. This method can be useful for further studies on the pharmacokinetic optimization and evaluating the druggability of nannozinone A including its efficacy and toxicity.

Keywords : Nannozinone A, LC-MS/MS analysis, pharmacokinetics

Introduction

Nannochelins A (Figure 1), a siderophores extracted from the Myxobacterium Nannocytis pusilla, strain MNa109131, was discovered to have cytotoxic activity as an iron complex.[1] Nannozinone A, a metabolite of nannochelins A, posseses a dihydropyrrolopyrazinone structure, and has antibacterial activity against some gram-positive bacteria, fungi, and viruses and has also shown to possess anti-cancer activity.[1-3] However, these biological activities of nannozinone A were previously only investigated in cell systems. The bioanalysis and pharmacokinetic properties of nanozinones A should be conducted during the early stages for investigating its in vivo activity and toxicity as well as its its potential as therapetic agent. Therefore, we aimed to develop and validate the bioanalysis of nanozinones A in mouse plasma samples and to investigate its pharmcokinetic properties when administered to ICR mice using our developed analytical method.

We used the liquid-liquid extraction (LLE) method for sample preparation since LLE has the advantage of lowering interferences from the sample matrix and increasing analyte sensitivity.[4] Moreover, our method was fully validated by observing the the U.S. Food and Drug Administration Guideline for Bioanalytical Method with regard to its linearity, selectivity, accuracy, precision, stability, recovery, and matrix effects.[5]

Experimental

Chemicals and reagents

Nannozinone A (Figure 1) were synthesized, with a purity of > 99.0%, and purtiy was confirmed by nuclear magnetic resonance spectroscopy and mass spectroscopy.[3] ^{13}C-Caffeine was used as the internal standard (IS), which was purchased from Sigma-Aldrich (St. Louis, MO, USA). The methyl *tert*-butyl ether (MTBE) was obtained from

[#]These authors contributed equally to this work
*Reprint requests to Min-Koo Choi and Young Taek Han
E-mail: minkoochoi@dankook.ac.kr and hany@dankook.ac.kr

Mallinckrodt Baker (Phillipsburg, NJ, USA). Acetonitrile, water, and methanol were purchased from Tedia (Fairfield, CT, USA). Formic acid was purchased from Sigma-Aldrich (St. Louis, MO, USA). All solvents and chemicals were of HPLC or reagent grade.

Preparation of stock and working solutions

Stock solutions were prepared by dissolving the nannozinone A in acetonitrile at a concentrations of 2 mg/mL. The nannozinone A working solutions were prepared by diluting the stock solution serially with acetonitrile and to achieve final concentrations of 10, 20, 50, 200, 500, 2000, 5000, and 10000 ng/mL. The ^{13}C-caffeine solution was prepared at a concentration of 20 ng/mL in water.

Preparation of standard calibration curve and quality control (QC) samples

The standard calibration curve and quality control (QC) samples were prepared by spiking 5 μL aliquot of the working solution with 45 μL aliquot of blank mouse plasma. The final concentrations of standard calibration curve and QC samples were 1, 2, 5, 20, 50, 200, 500, 1000 ng/mL and 1 (QC for lower limit of quantification; LLOQ QC), 3 (low QC), 100 (middle QC), 750 (high QC) ng/mL, respectively.

Sample preparation

The standard calibration curve and QC samples were added to 20 μL of ^{13}C-caffeine solution (20 ng/mL in water) and 400 μL of methyl *tert*-butyl ether. The mixture was vigorously vortexed for 10 min then centrifuged at 16,000 × *g* for 10 min. The supernatant was transferred to a clean tube and dried under a gentle stream of nitrogen. The residue was reconstituted in 150 μL of mobile phase and 5 μL aliquot of the solution and was injected into the LC-MS/MS system.

Instrument conditions

Nannozinone A in mouse plasma samples were analyzed using an Agilent 6430 triple quadrupole liquid chromatography-tandem mass spectrometry (LC-MS/MS) system (Agilent Technologies, Wilmington, DE, USA) equipped with an Agilent Infinity 1260 Infinite II HPLC system. Chromatographic separation was performed on a Luna C18 column (150 × 2.0 mm, 5 μm; Phenomenex, Torrance, CA, USA). Isocratic mobile phase consisting of mixture of water and acetonitrile (20:80, *v/v*) containing 0.1% formic acid was used at a flow rate of 0.2 mL/min with a column temperature maintained at 30 °C. The total run time for each injection was 4 min. The mass spectrometer was operated in the positive ion mode with multiple reaction monitoring (MRM) transitions at *m/z* 241.1→150.1 for nannozinone A and at *m/z* 198.2→140.0 for ^{13}C-caffeine with optimized fragmentor of 115 V and collision energy of 25 eV, respectively.

Method validation

Blank plasma samples from six different mouse were used for assessing selectivity. Signals of six blank plasma samples were compared to those of the corresponding LLOQ samples and IS. By plotting the ratio of the peak areas of the analyte and IS versus the concentrations of nannozinone A, the linearity of an eight-point standard calibration curve (1–1000 ng/mL) was generated using a least square linear regression utilizing $1/x^2$ as weighting factors. The extraction recovery and matrix effect was determined using three levels of QC samples (low-, middle-, and high QC) of nannozinone A and IS solution (20 ng/mL). The extraction recovery was calculated by comparing the peak areas of nannozinone A in QC samples through the extraction process with those in blank plasma extracts spiked with correstponding concentrations. The matrix effect was determined by dividing the peak areas in blank plasma extracts spiked with QC concentrations by those in neat solutions of the corresponding concentrations. The intra-day precision and accuracy were analyzed for the six replicates at four levels of QC samples (LLOQ-, low-, middle-, and high QC) on the same day. The inter-day precision and accuracy were determined by measuring the four levels of QC samples for six consecutive days. The bench-top stability was assessed by placing QC samples at 25°C for 5 h. The freeze-thaw stability was analyzed by comparing QC samples that underwent three freeze-thaw cycles (from -80°C to 25°C for 5 h as one cycle). Autosampler stability was evaluated by placing processed QC samples in the autosampler at 6°C for 24 h.

Pharmacokinetic study

All animal procedures were approved by the Animal Care and Use Committee of the Kyungpook National University (Permission no. 2019-0126). The male ICR mice (7-8 weeks old, 30-35 g) were purchased from the Samtako (Osan, Korea). Mice were acclimated to the animal facility of Kyungpook National University for a week with free access to food and water and fasted for 12 h prior to performing the pharmacokinetic experiments. Blood samples were collected via the Retro-Orbital plexus using heparinized collection tube at 0, 0.25, 0.5, 1, 2, 4, 8, and 24 h under anesthesia with isoflurane following the intravenous administration of nannozinone A (5 mg/kg dissolved in 1 mL mixture of DMSO : saline = 20:80 (*v/v*)) via the tail vein or following the oral administration of nannozinone A (30 mg/kg suspended in 2 mL of 0.5% carboxymethyl cellulose suspension) using oral gavage. The blood was centrifuged to separate the plasma at 16,000 × *g* for 1 min, and the plasma sample was stored at -80°C until analysis.

Data analysis

The pharmacokinetic parameters were determined by the non-compartmental analysis (WinNonlin® 2.0; Pharsight, Mountain View, CA, USA).[6] The area under the plasma

concentration-time curve from time 0 to the last measurement (AUC_{last}) was calculated using the linear trapezoidal method. The area under the plasma concentration-time curve from zero to infinity (AUC_{∞}) was calculated by the trapezoidal extrapolation method. Elimination rate constant (k) was the slope obtained from the plasma concentration-time curve. Half-life ($T_{1/2}$) was calculated as 0.693/k. Absolute oral bioavailability (BA) was calculated by dividing dose normalized AUC after intravenous injection (AUC_{IV}/$Dose_{IV}$) by dose normalized AUC after oral administration (AUC_{PO}/$Dose_{PO}$). Mean residence time (MRT), the average time a molecule stays in the body, was calculated by summing the total time in the body and dividing by the number of molecules. Maximum plasma concentration (C_{max}) and time to reach C_{max} (T_{max}) was read from the pharmacokinetic data. All data are expressed as the mean ± standard deviation (SD)

Results and Discussion

MS conditions

Nannozinone A and ^{13}C-caffeine (IS) showed optimal ionization in positive mode when monioted from the direct injection of nannozinone A and ^{13}C-caffeine into the mass spectrometer ionization source. MRM transition of nannozinone A was selected from the precursor ion ($[M+H]^+$, m/z 241.1) and the most frequent product ion (m/z 150.1), as shown in Figure 1. Similarly, MRM transition of ^{13}C-caffeine was selected from the precursor ion ($[M+H]^+$, m/z 198.2) and the most frequent product ion (m/z 140.0).[7]

Analytical method validation

Figure 2 shows the representative MRM chromatograms of double blank sample, zero blank sample, LLOQ sample (1 ng/mL), and plasma sample after oral administraion of nannozinone A. The retention times for nannozinone A and IS were 2.35 min and 1.99 min, respectively. The signal-to-noise (S/N) ratio of nannozinone A was more than 10.0 in the LLOQ samples and there was no significant matrix interference for the retention times of nannozinone A and IS in the blank samples compared with the LLOQ samples.

The extraction recoveries for nannozinone A were calculated at three levels of QC samples and were found to be high and reproducible, with a the range of extraction recoveries between 78.00-81.08% and a coefficient of variation (CV) 3.22-5.18% (Table 1), suggesting that the sample preparation method developed in this study was capable of efficiently extracting nannozinone A from mouse plasma. The matrix effects were between 70.56-96.49% with a CV of lower than 13.6%, indicating that co-eluting substances did not interfere with the ionization of the nannozinone A (Table 1).[5]

The standard calibration curves showed good linearity over the concentration range of 1–1000 ng/mL ($r^2 > 0.998$). Table 2 summarizes the intra- and inter-day precision and accuracy for nannozinone A from four levels of QC samples. The intra- and inter-day precision was found to

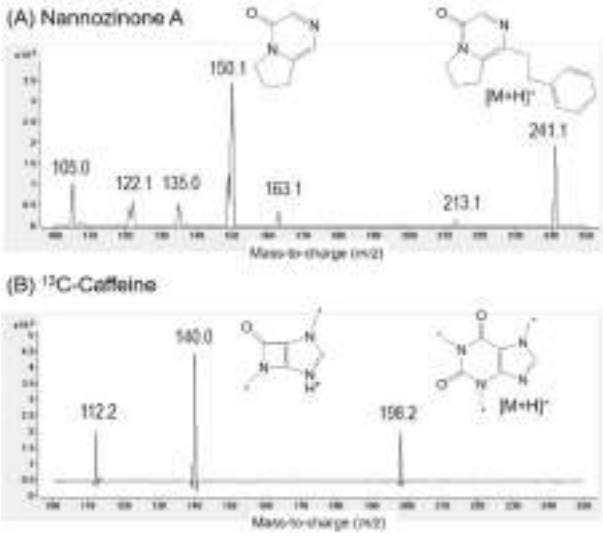

Figure 1. Product ion mass spectra of (A) nannozinone A and (B) ^{13}C-caffeine (IS).

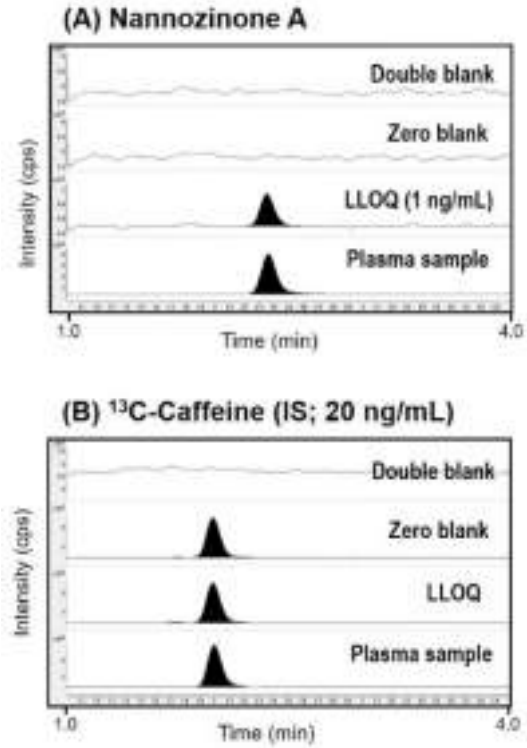

Figure 2. Representative MRM chromatograms of (A) nannozinone A and (B) ^{13}C-caffeine (IS) in mouse plasma of double blank, zero blank, LLOQ sample (1 ng/mL), and plasma sample at 2 h following oral administration of nannozinone A.

Table 1. Extraction recoveries and matrix effects of nannozinone A.

Analyte	Nominal concentration (ng/mL)	Extraction recovery (%)	CV (%)	Matrix effects (%)	CV (%)
Nannozinone A	3	81.08 ± 2.81	3.47	72.81 ± 1.70	2.33
	100	78.00 ± 2.51	3.22	70.56 ± 1.42	2.01
	750	79.18 ± 4.10	5.18	96.49 ± 13.1	13.6

Data represented as mean ± SD from six independent experiments.

Table 2. Intra- and inter-day precision and accuracy of nannozinone A in mouse plasma.

	Nominal concentration (ng/mL)	Measured concentration (ng/mL)	Precision (%)	Accuracy (%)
Intra-day	1	1.01 ± 0.09	9.31	101.04
	3	2.64 ± 0.13	4.91	87.87
	100	93.07 ± 12.61	13.55	93.07
	750	794.76 ± 63.86	8.04	105.97
Inter-day	1	1.02 ± 0.09	9.07	99.98
	3	3.00 ± 0.21	7.02	99.91
	100	97.39 ± 7.49	7.69	97.39
	750	756.22 ± 72.81	9.63	100.83

Data represented as mean ± SD from six independent experiments.

Table 3. Stability of nannozinone A in mouse plasma.

Nominal concentration (ng/mL)	Measured concentration (ng/mL)	Precision (%)	Accuracy (%)
Bench-top stability			
Low QC (3)	2.77 ± 0.18	6.34	92.23
High QC (750)	861.21 ± 21.14	2.45	114.83
Freeze-thaw stability			
Low QC (3)	2.94 ± 0.22	7.38	98.08
High QC (750)	788.34 ± 50.59	6.42	105.11
Autosampler stability			
Low QC (3)	3.17 ± 0.03	0.82	105.53
High QC (750)	747.25 ± 29.17	3.90	99.63

Data represented as mean ± SD from three independent experiments

range between 4.91 to 13.55% for nannozinone A and the intra- and inter-day accuracy was from 87.87 to 105.97%, which statisfies the acceptability criteria (less than 15%).[5] The results of the stability experiments are presented in Table 3. It was found that the accuracy of QC samples was within 114.83% for bench-top stability, within 105.11% for freeze-thaw stability, and within 105.53% autosampler stability. These results confirmed that nannozinone A is stable for up to 5 h on the bench-top at 25°C, and for over three freeze-thaw cycles, and for 24 h in an autosampler at 6°C.

Pharmacokinetic study

The plasma concentrations of nannozinone A after intravenous and oral administration in ICR mouse are shown in Figure 3, and the relevant pharmacokinetic parameters are listed in Table 4. The plasma concentrations of nannozinone A after intravenous injection declined sharply for 4 h, but the plasma concentrations of nannozinone A following oral administration showed a sharp decrease for 4 h and gradual decrease for 4-24 h, suggesting a high distribution kinetics. Consisently with this phenomenone, the clearance and volume of distribution of this compound were high (Table 4). It suggests that nannozinone A may undergo substantial metabolism or distribution, although the underlying mechanisms need to be further investigated.

The terminal half-life after oral administration of nannozinoe A was calculated as 8.0 ± 4.7 h, which was significantly longer compared to that of the intravenous injection (0.29 ± 0.12 h). Moreover, the mean absorption time, calculated by subtracting the mean residence time from the intravenous injection (MRT_{IV}) from the MRT_{PO} form the oral administration,[6,8] was calculated as 3.66 h, suggesting a long absorption time. The T_{max} value of nannozinone A was 15 min, indicating the rapid gastrointestinal

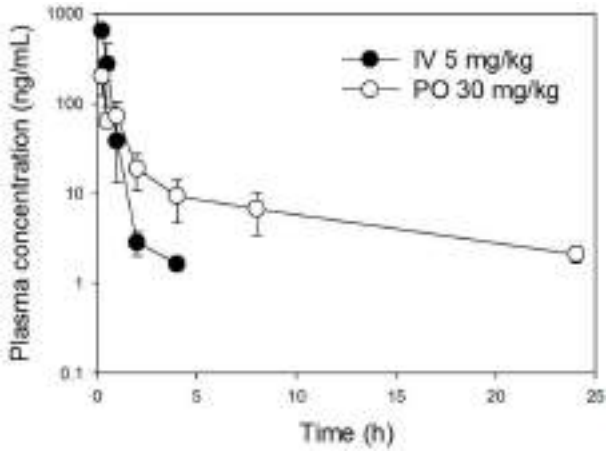

Figure 3. Plasma concentration-time profile of nannozinone A in mouse following an intravenous (IV, 5 mg/kg), and an oral (PO, 30 mg/kg) administration. Each data point represents the mean ± SD from four independent experiments.

Table 4. Pharmacokinetic parameters of nannozinone A following an intravenous (IV) and an oral (PO) administration in mouse.

Parameters	IV (5 mg/kg)	PO (30 mg/kg)
C_{max} (ng/mL)	-	205.37 ± 82.91
T_{max} (h)	-	0.25 ± 0.00
AUC_{last} (ng·h/mL)	535.67 ± 100.73	258.32 ± 83.93
AUC_{∞} (ng·h/mL)	536.73 ± 100.89	284.14 ± 87.86
$T_{1/2}$ (h)	0.29 ± 0.12	8.0 ± 4.7
MRT (h)	0.24 ± 0.08	3.9 ± 1.6
CL (mL/h/kg)	9561.30 ± 1762.99	-
$V_{d,ss}$ (mL/kg)	2269.34 ± 819.15	-
BA (%)	-	8.82

Data represents the mean ± SD from four independent experiments

absorption of nannozinone A.The AUC of intravenous and oral administration were calculated as 536.73 ± 100.89 and 284.14 ± 87.86 ng·h/mL, respectively, yielding a 8.82% of absolute oral bioavailability (BA). Taken together, once nannozinone A was given orally to mouse, nannozinone A was absorbed rapidly and stayed for long time but the extent absorbed was not great considering the low oral bioavailability. We should note the distinctive different half-life ($T_{1/2}$) after an intravenous and oral administration. The limited aqueous solubility of nannozinone A (4.44 ± 0.06 mg/mL), which was lower than oral dose (30 mg/kg/ 2 mL) and the long absorption time (3.66 h) could be attributed to the higher $T_{1/2, PO}$ than $T_{1/2, IV}$ since $T_{1/2, PO}$ could reflect the elimination and the delayed absorption.

Conclusions

In this study, we developed and validated a sensitive LC-MS/MS analytical method for nannozinone A in mouse plasma and we successfully applied this newly developed sensitive LC-MS/MS analytical method of nannozinone A to the pharmacokinetic evaluation of this compound. Consequently, the analytical method, and the pharmacokinetic features obtained from this study will facilitate the further preclinical investigation of nannozinone A.

Acknowledgements

This research has been done by the author(s) working at the Department of Pharmacy of Dankook University. Department of Pharmacy was supported by the Research-Focused Department Promotion Project as a part of the University Innovation Support Program 2020 to Dankook University.

References

1. Jansen, R.; Sood, S.; Mohr, K. I.; Kunze, B.; Irschik, H.; Stadler, M.; Mu?ller, R. *J. Nat. Prod.* **2014**, 77, 2545, DOI: 10.1021/np500632c.
2. Mulwa, L.; Stadler, M. *Microorganisms* **2018**, 6, 73, DOI: 10.3390/microorganisms6030073.
3. Ahn, S.; Li, F.; Han, Y. T. *Nat. Prod. Commun.* **2019**, 14, 1, DOI: 10.1177/1934578X1985749.
4. Kang, B.; Yoon, J.; Song, I. S.; Han, Y. T.; Choi, M. K. *Mass Spectrom. Lett.* **2019**, 10, 88, DOI: 10.5478/ MSL.2019.10.3.88.
5. Zimmer, D. *Bioanalysis* **2014**, 6, 13, DOI: 10.4155/ bio.13.298..
6. Kwon, M; Ji, H. K.; Goo, S. H.; Nam, S. J.; Kang Y. J.; Lee E.; Liu K. H.; Choi, M. K.; Song, I. S. *Drug Metab. Pharmacokinet.* **2017**, 32, 248, DOI: 10.1016/ j.dmpk.2017.05.005.
7. Wang, Y. H.; Mondal, G.; Butawan, M.; Bloomer, R. J.; Yates, C. R. *J. Chromatogr. B* **2020**, 1155, 122278, DOI: 10.1016/j.jchromb.2020.122278.
8. Jung, D.; Mroszczak, E.; Bynum, L. *Eur J Clin Pharmacol.* **1988**, 35, 423.

Vol. 12, No. 1, 2021
ISSN 2233-4203/ e-ISSN 2093-8950
ARTICLE www.msletters.org | Mass Spectrometry Letters

Boron Detection Technique in Silicon Thin Film Using Dynamic Time of Flight Secondary Ion Mass Spectrometry

M. Abul Hossion[1]* and Brij M. Arora[2]

[1]*Department of Physics, BSMR Maritime University, Dhaka 1216, Bangladesh*
[2]*Department of Physics, University of Mumbai, Mumbai 400098 India*

Received March 5, 2021, Revised March 25, 2021, Accepted March 25, 2021
First published on the web March 31, 2021; DOI: 10.5478/MSL.2021.12.1.26

Abstract : The impurity concentration is a crucial parameter for semiconductor thin films. Evaluating the impurity distribution in silicon thin film is another challenge. In this study, we have investigated the doping concentration of boron in silicon thin film using time of flight secondary ion mass spectrometry in dynamic mode of operation. Boron doped silicon film was grown on i) p-type silicon wafer and ii) borosilicate glass using hot wire chemical vapor deposition technique for possible applications in optoelectronic devices. Using well-tuned SIMS measurement recipe, we have detected the boron counts 10^1~10^4 along with the silicon matrix element. The secondary ion beam sputtering area, sputtering duration and mass analyser analysing duration were used as key variables for the tuning of the recipe. The quantitative analysis of counts to concentration conversion was done following standard relative sensitivity factor. The concentration of boron in silicon was determined 10^{17}~10^{21} atoms/cm^3. The technique will be useful for evaluating distributions of various dopants (arsenic, phosphorous, bismuth etc.) in silicon thin film efficiently.

Keywords : ToF-SIMS, HWCVD, boron concentration, p-type silicon, RSF, thin film.

Introduction

Secondary ion mass spectrometry is an established method for identification and quantification of isotopes and elements on the top surface or below the surface of a solid sample. Dopant concentrations and their depth distribution are of major importance for the electrical performance of semiconductor devices such as transistors and optoelectronic devices such as sensors, photovoltaic devices etc. Due to the high detection sensitivity, secondary ion mass spectrometry (SIMS) is widely used for the determination of impurity concentration of dopant materials in silicon thin films.[1] Since its inception in 1949, the major improvement in instrumentation came in 1980-2013.[2] Depending on the mass analyser, available types of instrumentation of SIMS are i) Magnetic sector ii) Quadruple and iii) Time of Flight (ToF).[3,4] The data acquisition of SIMS is performed in two distinct modes of operation, the static and dynamic modes. In the static mode, materials from several points of the top surface of a sample is sputtered. In the dynamic mode, materials from a single point on the top surface of a sample is sputtered to produce a crater which provides in-depth data of elements.[5] The mass spectrum is obtained by rastering the top of the sample surface using a pulsed primary ion gun followed by sputtering the region using secondary ion gun.[6]

The detection, interpretation and identification of the isotope of interest is crucial as the detector detects a cluster of different isotopes.[7,8] The process becomes further challenging for thin film devices such as transistors, sensors and photovoltaic devices, where the distribution of dopants dictates the performance of the device.[9-11] An established method for the data analysis is to use a reference sample of known impurity concentration obtained from ion implantation techniques.[12] The availability of the ion implantation facility and reference samples limits the characterization process.

In this article, we demonstrate, how by using well-tuned conditions, the detection of Boron (B) in silicon thin film can be performed by time of flight secondary ion mass spectrometry (ToF-SIMS) using dynamic mode of operation efficiently. In most works using SIMS measurement, only the final results are tabulated. In this work, primary ion beam raster area, secondary ion beam sputtering area, sputtering duration and mass analyser

*Reprint requests to M. Abul Hossion, orcid.org/0000-0002-3199-1682
E-mail: abulhossion.phy@bsmrmu.edu.bd

analysing duration were used as key variables for well-tuned recipe are specified. The data acquisition and interpretation were followed by conversion of counts to concentration using relative sensitivity factor (RSF) procedure.

Experimental

Sample preparation

Samples used in this work were thin films synthesized by hot wire chemical vapor deposition (HWCVD) technique, widely used because of its simplicity of operation. Initially, thin ~20 nm nucleation layer of intrinsic silicon was grown on i) p-type silicon (100) single side polished wafer (89-Boron) and ii) alkali free borosilicate corning 7059 glass (88-Boron), as substrate, at 400°C with a gas ratio SiH_4:H_2 = 1:20 for 100 s. Filament temperature was kept at 1900°C at all stages. After the nucleation stage, a mixture of silane (SiH_4) and hydrogen (H_2) were used as process gas with a ratio of SiH_4:H_2 = 5:15 for 20 min at 600°C substrate temperature. The intrinsic silicon film was annealed at this stage under 20 sccm (standard cubic centimetre per minute) of H_2 flow for 30 min followed by a H_2 soaking, during cooling the sample from the growth temperature to a lower temperature of 200°C for another 45 min.[13] These poly crystalline intrinsic silicon films have (220) preferred crystalline orientation.[14] At this stage boron containing gas (5% diborane in hydrogen) was introduced with a gas ratio SiH_4:5%B_2H_6:H_2 = 1:1:20 for 10 min to grow the amorphous boron doped layer. The thicknesses of intrinsic silicon film and boron doped film are 800 nm and 100 nm respectively, estimated from cross sectional transmission electron microscopy.[15] A boron diffused silicon wafer was used as reference to validate the data acquisition technique and comparison of boron concentration of this study to values shown in other literature.[16-18] The reference boron diffused sample was prepared using standard diffusion furnace at 1000°C for 20 min on 2 inch diameter p-type silicon wafer. This diffusion process allowed the boron atoms to diffuse into the Si wafer to a depth of about 1000 nm.

Depth profile analysis

The total crater depth was measured using Veeco Dektak 150 surface profiler and the data given in Figure 1 and Table 1. The sputtering rate was obtained from the total crater depth divided by the total sputtering duration. The sputtering rate for reference boron diffused silicon wafer is 0.34 nm/s, where the crater depth is 1416 nm as shown in Figure 1(i) and total sputtering duration is 4120 s. The sputtering rate for 89-Boron doped intrinsic silicon thin film using HWCVD is 0.39 nm/s, where the total crater depth is 1266 nm as shown in Figure 1(ii) and total sputtering duration is 3260 s. The duration of mass analyser analysing duration was deducted from the total time to calculate actual sputtering duration.

TOF-SIMS data acquisition

The detection of secondary ions is carried out using a mass analyser based on the time of flight principle: ions are accelerated into a flight tube and measures the exact flight duration. Thus, ions are separated by the time of flight analysis from which a mass spectrum is generated.[19,20]

To measure the secondary ion counts, the PHI nano TOF II TRIFT was used from Physical Electronics, MN, USA. In this process, a 10 ns pulsed liquid metal ion gun (LMIG) uses Gallium sources to produce (Ga^+) ions as primary ion

Table 1. Veeco Dektak 150 surface profiler data for the crater depth and the scanning length.

Sample Name	Cursor Position	Cursor Width (mm)	X-axis position (mm)	Crater Length (mm)	Y-axis position (nm)	Crater Depth (nm)
Reference boron	Left	0.1668	0.9212	1.2574	111.32	1416.74
	Middle	0.2113	1.5499		-1381.18	
89-Boron	Left	0.1668	0.2285	1.6328	42.1655	1266.16
	Middle	0.2039	1.0449		-1242.14	

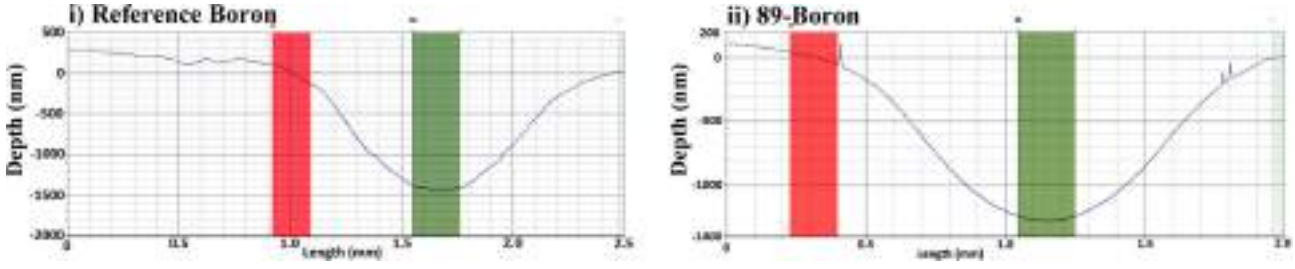

Figure 1. The surface profile of the total depth of the crater for i) reference boron diffused silicon wafer is 1416 nm and ii) 89-Boron doped intrinsic silicon thin film using HWCVD is 1266 nm measured using Veeco Dektak 150 surface profiler.

Table 2. ToF-SIMS scanning parameters for the detection of boron isotope (^{11}B) and silicon isotope (^{30}Si) in silicon thin film using oxygen ion (O^{2+}) sputtering gun.

Sample Name	Boron thin film thickness (nm)	Sputtering beam current (A)	Sputtering beam Energy (kV)	Sputtering beam raster area (μm^2)	Sputtering duration (s)	Mass analyser analysing duration (s)
Reference boron	1000	8.4×10^{-7}	3	200 × 200	20	60
89-Boron	100			400 × 400		

Table 3. Part of data for the conversion of ToF-SIMS data to concentration-depth profile. The complete data set is provided as supporting information.

Cycle number (A)	Sputtering Duration (s) (B)	Total Time (s) (A×B)	Sputtering rate (nm/s) (C)	Crater depth (nm) [(A×B)C]	Measured Intensity of ^{11}B isotope (counts)	Measured Intensity of ^{30}Si isotope (counts)	Boron concentration (atoms/cm^3)
i) Reference Boron diffused silicon wafer							
1	20	20	0.34	6.88	4333	113765	8.26E+19
2	20	40	0.34	13.75	8470	138927	1.32E+20
3	20	60	0.34	20.63	11015	140310	*1.70E+20
ii) 89-Boron doped intrinsic silicon thin film using HWCVD							
1	20	20	0.39	7.77	50365	33616	3.25E+21
2	20	40	0.39	15.53	58367	46138	2.75E+21
3	20	60	0.39	23.30	56577	47072	2.61E+21

*Using equation-1, $C_B = 7\times10^{22}\times0.031\times(\frac{11015}{140310}) = 1.720\times10^{20}$ atoms/cm^3

beam to ionise the surface molecules.[21] The beam energy was kept 30 kV with a beam current of 8×10^{-9} A and the raster size 200 × 200 μm^2.[22] The oxygen ion (O^{2+}) gun was used as sputtering tool to produce positive secondary ions.[23]

In this study, the boron isotope (^{11}B) and silicon isotope (^{30}Si) were detected. The scanning parameters are given in Table 2. For sample with lower impurity concentration, the ion counts can be increased by allowing the mass analyser to analyse for longer duration. The tuning was also performed on the sputtering area. For thinner sample, a larger sputtering area was used where, for thicker sample, a smaller sputtering area allows the sputtering to occur deeper. The sputtering beam raster area given in the Table 2 was selected by performing the sputtering at different locations on the sample with the variation of the raster size range 100 × 100 μm^2 to 600 × 600 μm^2.

Results and Discussion

The ToF-SIMS signal is interpreted using relative sensitivity factor for Boron Counts to concentration conversion. The concentration of boron (C_B) in silicon is calculated using the following equation 1,

$$C_B = RSF_{B(Si)} \times \%^{30}Si \times (\frac{I_{B(Si)}}{I_{30Si}}) \quad (1)$$

Here, C_B is Concentration of boron in silicon, $RSF_{B(Si)}$ is relative sensitivity factor of boron in silicon,[6] $\%^{30}Si$ is fractional isotope abundance of ^{30}Si in silicon,[24] $I_{B(Si)}$ is intensity of boron isotope (^{11}B) counts and I_{30Si} is intensity of silicon isotope (^{30}Si) counts with oxygen (O^{2+}) gun using ToF-SIMS. Table 3 shows the part of data used in the Boron counts to concentration conversion calculation. The complete data table is provided with the article as supporting information.

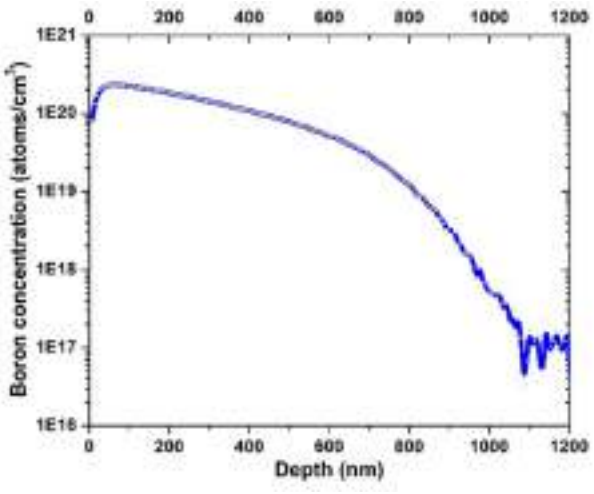

Figure 2. Boron concentration – depth curve of Reference boron diffused silicon wafer

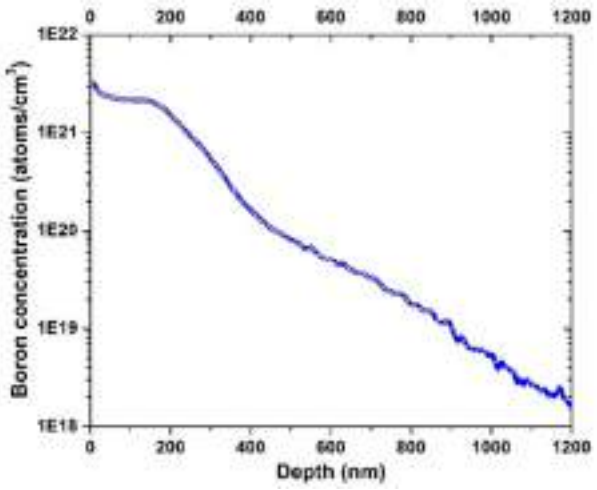

Figure 3. Boron concentration – depth curve of 89-Boron doped intrinsic silicon thin film using HWCVD.

Table 3 is used to plot Boron concentration versus crater depth curve for i) Reference Boron and ii) 89-Boron as shown in Figure 2 and 3 respectively. Figure 2 shows the concentration of boron, diffused in p-type silicon wafer for Reference Boron sample. The concentration at the top surface of the wafer is 2×10^{20} atoms/cm^3 which decreases with the depth. Figure 3 shows the concentration of boron in intrinsic silicon thin film grown using HWCVD. The concentration is 3.25×10^{21} atoms/cm^3 at the top amorphous layer. This remain uniform over the top 150 nm and then starts to decrease as it reaches the lower intrinsic silicon thin film. This shows that the intrinsic silicon film also gets diffused by boron atoms. This may happen due to the reason that the out-diffusion of boron atoms from the wafer at high (600^{o}C substrate and 1900^{o}C filament) process temperature contaminated the intrinsic silicon film.[25-27] The Boron concentration in the reference boron diffused silicon wafer shown in Figure 2 is 1×10^{20} atoms/cm^3 at 400 nm which is in close agreement with the data found in other measurements.[28-30] At room temperature the boron concentration in 200 μm silicon wafer published in other literature was found 7×10^{20} atoms/cm^3 using hot probe method.[31]

Conclusions

The concentration of boron in silicon thin film was measured using versatile ToF-SIMS technique. Relative sensitivity factor was used to interpret the ToF-SIMS data of boron isotope and silicon matrix element. The boron in silicon detected on the top surface of amorphous boron doped silicon thin film was 3.25×10^{21} atoms/cm^3 where 1×10^{18} atoms/cm^3 was detected at one-micron depth. The tuning of i) sputtering area to the thickness of thin film and ii) mass analyser analysing duration to the boron counts, provides an efficient route for the detection of dopants in the silicon thin film. The results of this study will be useful for the detection and quantification of impurities in wide area of thin films using complex ToF-SIMS technique.

Supporting Information

Supporting information is available at https://drive.google.com/file/d/1ME73GRSTLKC--v8qPjm68lpIePQtW4Dd/view?usp=sharing.

Acknowledgements

The authors thank Yuriy Kudriavtsev, Center for Research and Advanced Studies of the National Polytechnic Institute, Apodaca, Mexico, for the suggestions in data interpretation. The authors also thank to Dr. C. S. Harendranath, Principle research scientist, Sophisticated analytical instrument facility (SAIF), Indian Institute of Technology Bombay, Mumbai, India, for providing necessary laboratory facilities. The authors are grateful to Mr. Subhash Lokhre and Mr. Nilesh Marle for their active participation during measurement process. We are also grateful to HWCVD system team Anjum A., Poonam K., and Raorane, Centre of Excellence in Nanoelectronics (CEN), Indian Institute of Technology Bombay, Mumbai, India.

Author contributions

Both the authors Abul Hossion (A.H) and Brij Mohan Arora (B.M.A) participated in the conceptualization, designing methodology, analysis, interpretation, discussion and improvement of the manuscript of the experimental data on ToF-SIMS study on boron doped silicon film. A.H. collected and analysed the data followed by the manuscript preparation while B.M.A does the review, editing, supervision and funding acquisition. All the figures and images are prepared by A.H. Both the authors have read and agreed to the published version of the manuscript.

Funding

This research was funded by Centre of Excellence in Nano electronics (CEN) of the Indian Institute of Technology, Bombay, Mumbai, India.

Conflicts of interest

The authors declare no conflict of interest. The funders had no role in the design of the study; in the collection, analysis, or interpretation of data; in the writing of the manuscript, or in the decision to publish the results.

References

1. van der Heide, P. *Secondary Ion Mass Spectrometry: An Introduction to Principles and Practices 1st ed.*, Wiley & Sons: New York, **2014**.
2. Hofmann, J. P.; Rohnke, M.; Weckhuysen, B. M.; *Phys. Chem. Chem. Phys.* **2014**, 16, 5465, DOI: 10.1039/C3CP54337D.
3. Riviere, J. C.; Myhra, S.; Myhra, S. *Handbook of Surface and Interface Analysis: Methods for Problem-Solving 2nd ed.,* CRC Press, New York, **2009**, https://doi.org/10.1201/9781420007800.
4. Wilson, R. G. *Secondary ion mass spectrometry: a practical handbook for depth profiling and bulk impurity analysis.* Wiley & Sons: New York, **1989**.
5. Benninghoven, A.; Rudenauer, F. G.; Werner, H.W. *Secondary Ion Mass Spectrometry: Basic Concepts, Instrumental Aspects, Applications and Trends*, Wiley & Sons: New York, **1987**.
6. Stevie, F. *Secondary Ion Mass Spectrometry: Applications for Depth Profiling and Surface Characterization.* Momentum Press, New York, **2015**.
7. Priebe, A.; Xie, T.; Bürki, G.; Pethö, L.; Michler, J. J. *Anal. At. Spectrom*. **2020**, 35, 1156, DOI: 10.1039/C9JA00428A.
8. Collin, M.; Gin, S.; Jollivet, P.; Dupuy, L.; Dauvois, V.; Duffours, L.; *NPJ Mater. Degrad*. **2019**, 3, 1, DOI: 10.1038/s41529-019-0076-3.
9. Sandow, C.; Knoch, J.; Urban, C.; Zhao, Q.-T.; Mantl, S. *Solid State Electron*. **2009**, 53, 1126, DOI: 10.1016/j.sse.2009.05.009.
10. Kim, E.-Y.; Kim, J. *Adv. Mater. Sci. Eng.* **2013**, 2013, e974507. DOI: 10.1155/2013/974507.
11. Fang, W.; Ni, Z.; Wang, P.; Xiang, C.; Sun, T.; Zhang, J.; Wang, R.; Yang, J.; Yang, Y. *J. Mater. Sci: Mater. Electron.* **2020**, 31, 6398, DOI: 10.1007/s10854-020-03196-y.
12. Eswara, S.; Pshenova, A.; Lentzen, E.; Nogay, G.; Lehmann, M.; Ingenito, A.; Jeangros, Q.; Haug, F.-J.; Valle, N.; Philipp, P.; Hessler-Wyser, A.; Wirtz, T. *MRS Commun.* **2019**, 9, 916, DOI: 10.1557/mrc.2019.89.
13. Kaur, G.; Hossion, M. A.; Kulasekaran M; Arora, B. M. *IEEE 40th Photovoltaic Specialist Conference (PVSC)* **2014,** 1326, DOI: 10.1109/PVSC.2014.6925162.
14. Hossion, M. A., Arora, B. M. *IEEE 40th Photovoltaic Specialist Conference (PVSC)* **2014,** 1292, DOI: 10.1109/PVSC.2014.6925153.
15. Hossion, M. A.; Arora, B. M. *Int. J. Thin Film Sci. Tech.* **2020**, 9, 37, DOI: 10.18576/ijtfst/090106.
16. Fu, J.; Chen, K.; Chang, S.; Zhi, K.; Gao, X.; Wei, H.; Dan, Y. *AIP Adv.* **2019**, 9, 125219, DOI: 10.1063/1.5134118.
17. Dutta, S.; Pandey, A.; Saxena, G.; Raman, R.; Dhaul, A.; Pal, R.; Chatterjee, R. *J. Mater. Sci.: Mater. Electron.* **2012**, 23, 1569, DOI: 10.1007/s10854-012-0630-z.
18. Mirabella, S.; De Salvador, D.; Napolitani, E.; Bruno, E.; Priolo, F. *J. Appl. Phys.* **2013,** 113, 031101. https://doi.org/10.1063/1.4763353
19. Guilhaus, M. *J. Mass Spectrom.* **1995**, 30, 1519, DOI: 10.1002/jms.1190301102
20. Douglas, M. A.; Chen, P. J.; *Surf. Interface Anal*. **1998**, 26, 984, DOI: 10.1002/(SICI)1096-9918(199812)26:13<984::AID-SIA446>3.0.CO;2-K.
21. Bayly, A. R.; Waugh, A. R.; Anderson, K. *Nucl. Instrum. Methods Phys. Res*. **1983**, 218, 375, DOI: 10.1016/0167-5087(83)91009-8.
22. Kia, A. M.; Haufe, N.; Esmaeili, S.; Mart, C.; Utriainen, M.; Puurunen, R. L.; Weinreich, W. *Nanomaterials* **2019,** 9, 1035, DOI: 10.3390/nano9071035.
23. Beljakowa, S.; Pichler, P.; Kalkofen, B.; Hübner, R. *Phys. Status solidi A* **2019**, 216, 1900306, DOI: 10.1002/pssa.201900306.
24. Meija, J.; Coplen, T. B.; Berglund, M.; Brand, W. B.; De Bièvre, P.; Gröning, M.; Holden, N. E.; Irrgeher, J.; Loss, R. D.; Walczyk, T.; Prohaska, T. *Pure Appl. Chem.* **2016**, 88, 3, 265, DOI: 10.1515/pac-2015-0305.
25. Kurachi, I.; Yoshioka, K. *Int. J. Photoenergy* **2016**, 8183673, DOI: 10.1155/2016/8183673.
26. Perova, T. S.; Nolan-Jones, M.; McGilp, J.; Gamble, H. S. *J. Mater. Sci.: Mater. Electron.* **2016,** 27, 6292, DOI: 10.1007/s10854-016-4561-y.
27. Lill, P. C.; Dahlinger, M.; Köhler, J. R. *Materials* **2017**, 10, 189, DOI: 10.3390/ma10020189.
28. Park, C. J.; Kim, K. J.; Cha, M. J.; Lee, D. S. *Analyst* **2000**, 125, 493, DOI: 10.1039/A909215C.
29. Cojocaru-Mirédin, O.; Cadel, E.; Deconihout, B.; Mangelinck, D.; Blavette, D. *Ultramicroscopy* **2009**, 109, 649, DOI: 10.1016/j.ultramic.2008.09.008.
30. Pisonero, J.; Lobo, L.; Bordel, N.; Tempez, A.; Bensaoula, A.; Badi, N.; Sanz-Medel, A. *Sol. Energy Mater. Sol. Cells* **2010**, 94, 1352, DOI: 10.1016/j.solmat.2010.04.002.
31. Akter, N.; Afrin, S.; Hossion, A.; Kabir, K.; Akter, S.; Mahmood, Z. *Int. J. Adv. Mater. Sci. Eng.* **2015**, 4, 13, DOI: 10.14810/ijamse.2015.4402.

Author Guidelines

Aims and Scope

Mass Spectrometry Letters publishes brief letters (maximum length of 4 pages), technical notes, articles, reviews, and tutorials on fundamental research and applications in all areas of mass spectrometry. The manuscripts can be either invited by the editors or submitted directly by authors to the journal editors. Mass Spectrometry Letters topical sections are diverse, covering ion chemistry in a broad sense; gas-phase thermodynamics or kinetics; theory and calculations related with mass spectrometry or ions in vacuum; ion-optics; analytical aspects of mass spectrometry; instrumentations; methodology developments; ionization methods; proteomics and its related research; metabolomics and its related research; bioinformatics; software developments; database development; biological research using mass spectrometry; pharmaceutical research by mass spectrometry; food sciences using mass spectrometry; forensic results using mass spectrometry; environmental mass spectrometry; inorganic mass spectrometry; chromatography-mass spectrometry; tandem mass spectrometry; small molecule research using mass spectrometry; TOF-SIMS, etc. The scope of Mass Spectrometry Letters is not limited to the above-mentioned areas, but includes ever-expanding areas related directly or indirectly to mass spectrometry. Criteria for publication are originality, urgency, and reportable values. Short preliminary or proof-of-concept results, which will be further detailed by the following submission to other journals, are recommended for submission.

The publication frequency

Mass Spectrometry Letters will be published at least four times a year; 31th March, 30th June, 30th September, 31th December every year are the scheduled publishing dates. The publication frequency is subjected to future change, which should be advised by the Editorial board meeting's decisions.

The publication charge

All the papers will be published for free without any payment of page charge or article processing charge and the access to the papers in Mass Spectrometry Letters is also free to the public in general through the homepage of the journal. The publication cost will be covered by the Korean Society for Mass Spectrometry. The printed journal issue will be provided to the Korean Society for Mass Spectrometry members who have completed the annual membership fee payment.

The copyright

Referee Reviews

Submitted manuscripts are subjected to review by at least 2 referees selected by the editors. The authors can recommend preferred potential reviewers with the names and e-mail addresses. Note that the editor retains the sole right to decide whether or not the suggested reviewers are used.

Conflict of interest

All authors are requested to disclose any actual or potential conflict of interest including any financial, personal or other relationships with other people or organizations within three years of beginning the submitted work that could inappropriately influence, or be perceived to influence, their work.

Submission declaration and verification

Submission of an article implies that the work described has not been published previously (except in the form of an abstract or as part of a published lecture or academic thesis), that it is not under consideration for publication elsewhere, that its publication is approved by all authors and tacitly or explicitly by the responsible

authorities where the work was carried out, and that, if accepted, it will not be published elsewhere in the same form, in English or in any other language, including electronically without the written consent of the copyright-holder. To verify originality, your article may be checked by the originality detection software.

Research/publication ethics and research/publication malpractice statement

For the policies on the research and publication ethics not stated in these instructions, international standards for editors and authors (http://publicationethics.org/international-standards-editors-and-authors) can be applied.

Language and language services

The manuscript should be prepared in good English (American or British usage is accepted, but not a mixture of these). English language proof-reading service is recommended before publication.

Submission

Submission to this journal proceeds totally online and you will be guided stepwise through the creation and uploading of your files.

Manuscript Types

Mass Spectrometry Letters publishes several types of articles: letter, technical note, article, review, and tutorial.

· **Review.** A comprehensive overview on a topic in mass spectrometry. There is no restriction in length.

· **Article.** A full-length article presenting important new research results. The length of the articles should not exceed ten printed pages.

· **Technical note.** A short description of a novel apparatus of technique. The length of technical notes should not exceed three printed pages.

· **Letter.** A short report on any subject in mass spectrometry, requiring urgency, timeliness, and scientific significance. The length of letters should not exceed four printed pages.

· **Tutorial.** A tutorial is an educational exposition covering recent trends and basic knowledge in mass spectrometry. There is no restriction in length

All manuscripts for publication in Mass Spectrometry Letters, except review and tutorial, should include Title, Authors, Abstract, Introduction, Experimental section, Results and Discussion, Conclusions, Acknowledgments, and References.

Preparation of Manuscripts

All the manuscripts for publication in Mass Spectrometry Letters should be prepared in English. Authors are strongly recommended to use the manuscript template (Manuscript Template) provided from the Mass Spectrometry Letters website.

1) Manuscript type

The type of a manuscript should be specified in the cover letter.

2) Title

The title should be concise and informative. Authors are strongly recommended to limit the title to 250 letters including space, and to avoida bbreviations and formulae wherever possible. A short running title consisting of less than 70 letters including space should be provided by authors.

3) Authors

List full names of all authors (given names first and surnames last) followed by the authors' affiliations and addresses where the actual work was carried out. Superscript numbers are labeled after the authors' names and in front of the appropriate affiliations. Specify current addresses, if necessary, as footnotes. Provide the full postal address of each affiliation including the country name. Corresponding author(s) should beindicated with asterisk symbols. The email address(es) of corresponding author(s) are additionally required in the manuscript.

4) Abstract

The abstract should not exceed 250 words. It should be a single paragraph which summarizes the content of the article.

5) Introduction

The introduction should state the purpose and the backgrounds of thework. It may include appropriate citations of previous works with brief summaries. Do not include or summarize current findings in this section.

6) Experimental section

Authors should provide details on experimental procedures including the model names, the manufactures of instruments, and reagents, so that the works are reproducible elsewhere by readers.

7) Results and discussion

Authors should provide the results of the work with clear and concise manners. Authors should discuss the significance of observations, measurements, or computations.

8) Conclusion

A brief summary should be provided in conclusions.

9) Acknowledgements

Provide a list of financial supports and individuals whom to be acknowledged.

10) References

Literatures to be cited should be numbered by order of appearance in the manuscript. The corresponding texts should be indicated with superscripted Arabic numbers (e.g., 1). The reference format must follow the examples provided below. Unpublished results are not allowed in the reference list with an exception of the literatures accepted for publication as "in press".

<Journals>

Hong, E. S.; Yoon, H.-J.; Kim, B.; Yim, Y.-H.; So, H.-Y.; Shin, S. K. *J. Am. Soc. Mass Spectrom.* **2010**, 21, 1245, DOI: 10.1016/j.jasms.2010.03.035

<Books>

Bunker, P. R.; Jensen, P. Molecular Symmetry and Spectroscopy, 2nd ed.. NRC Research Press: Ottawa, 1998.

Zare, R. N. Angular Momentum, Wiley: New York, 1998.

<Software>

Werner, H. J.; Knowles, P. J.; Lindh, R.; Manby, F. R.; Schutz, M. MOLPRO, version 2006. 1., A package of ab initio Programs; See http://www.molpro.net.

<Proceedings>

Bensaude-Vincent, B. The New Identity of Chemistry as Biomimetic and Nanoscience; 6th International Conferenceon the History of Chemistry, Leuven (Belgium), August 28 - September 1, 2007, p 53.

11) Equations and math formulae

Equations and math formulae should be prepared by Microsoft Equation 3.0 (or a later version). All the equations and math formulae should be numbered by order of appearance in the manuscript with Arabic numbers.

12) Tables

Tables should be numbered by order of appearance in the manuscript with Arabic numbers. Each table should have a brief title. Footnotes may be placed, if necessary, to supplement the tables. Avoid vertical rules. The size of table should fit the MSL's page (16.5 cm × 22.5 cm).

13) Figures

Figures should be numbered by order of appearance in the manuscript with Arabic numbers. Each figure should have a brief title followed by a brief description, which consists of one or two sentences. Sub-numbering is possible with lowercase alphabets (e.g., a, b, etc.), if necessary. The resolution of a figure should be better than 600 dpi. JPEG (jpg, Joint Photographic Expert Group) format is recommended.

14) Units

SI units rather than conventional units should be used for reporting measures. Information regarding on SI units can be found at https://www.nist.gov/pml/weights-and-measures/metric-si/si-units.


KSMS
Korean Society for Mass Spectrometry